First principles study of the diatomic charged fluorides $MF^{\pm}$, M=Sc, Ti, V, Cr, and Mn

Stavros Kardahakis, Constantine Koukounas, and Aristides Mavridis[a)]
Laboratory of Physical Chemistry, Department of Chemistry, National and Kapodistrian University of Athens, P.O. Box 64 004, 15710 Zografou, Athens, Greece

(Received 1 September 2004; accepted 27 October 2004; published online 20 January 2005)

Employing multireference configuration interaction and coupled-cluster methods in conjunction with quantitative basis sets, we have explored the electronic structure of the charged diatomic fluorides $MF^{\pm}$, where M=Sc, Ti, V, Cr, and Mn. In addition, and in order to complete our recently published work on the neutral diatomic fluorides MF, M=Ti–Mn [C. Koukounas, S. Kardahakis, and A. Mavridis, J. Chem. Phys. **120**, 11500 (2004)], we have also examined the ground ($X\,^1\Sigma^+$) and the first excited state ($\alpha\,^3\Delta$) of neutral ScF. For the entire anionic MF^- series and the cations ScF^+, VF^+, and MnF^+, no experimental or theoretical results of any kind have been reported so far in the literature. For the charged $MF^{\pm}$ sequence we have investigated a total of 43=29(MF^+)+14(MF^-) states, reporting potential energy curves, energetics, and common spectroscopic parameters. Two are the most interesting conclusions of the present work. (a) The Coulombic binding character of MF^+ cations, i.e., the conformity of their equilibrium description to $M^{2+}F^-$ and (b) the atypical bonding of the MF^- anions and their surprisingly high dissociation energies (up to 85 kcal/mol for the $X\,^2\Delta$ state of ScF^-). Considering the complexities of these chemically ''simple'' systems, our results on ScF, TiF^+, and CrF^+ are in very good agreement with the limited experimental findings. © *2005 American Institute of Physics.* [DOI: 10.1063/1.1834912]

I. INTRODUCTION

Continuing our previous investigation of the first row transition metal diatomic fluorides MF, M=Ti, V, Cr, and Mn,[1] we focus our attention presently on the cationic and anionic series MF^+ and MF^-, where M=Sc, Ti, V, Cr, and Mn. The challenging difficulties and the inherent complexity of the first row transition metal containing compounds, and the frequently insurmountable difficulties of obtaining reliable *ab initio* results of even diatomic MX molecules, are well known.[1,2] The situation becomes even more compounded in cases, as the present one, where experimental results are scarce (MF^+), or are completely lacking (MF^-). These reasons and our recent experience with the neutral MF series[1] provided the motivation for a thorough and systematic investigation of the $MF^{\pm}$ sequence, M=Sc to Mn.

As was mentioned the information concerning the MF^+ species is very limited: ScF^+, VF^+, and MnF^+ are both experimentally and theoretically unexplored. Pradeep *et al.*[3] were, perhaps, the first to examine the MF_n^+ cations (M=Ti, Cr, Fe, Mo, and W, n=1–5) as scattered products of low-energy (<100 eV) metal ions off a fluorinated monolayer surface. In 1998 Focsa *et al.*,[4] by means of velocity modulation laser spectroscopy, asserted that the ground state of TiF^+ is $^3\Phi$ (but see below). Their work provided for the first time spectroscopic numerical results on the $X\,^3\Phi$ and a [17.6] $^3\Delta$ state of TiF^+. They reported equilibrium bond distances r_e=1.7800(1), 1.7509(1) Å, harmonic and anharmonic frequencies $\omega_e/\omega_e x_e$=781(6)/3.4(2), 880(8)/3.8(2) cm^{-1}, rotational-vibrational constants α_e=0.002 285(55), 0.002 287(55) cm^{-1}, as well as spin–orbit coupling constants A_e=63.2(8), 59.2(5) cm^{-1}, for the $^3\Phi$ and $^3\Delta$ states, respectively.[4]

Schröder and co-workers[5] using charge-stripping mass spectrometry determined the vertical ionization energies of TiF^+ (15.2±0.3 eV) and TiF^{2+} (28±3 eV). The same workers employing the coupled cluster singles and doubles with a perturbative treatment of connected triples methodology (RCCSD(T)/[$6s5p4d2f/_M 6s5p3d/_F$]), obtained binding energies D_e, bond distances r_e, and energy separations T_e for TiF^+ ($^3\Phi$, $^3\Sigma^-$), TiF^{2+} ($1\,^2\Delta$,$2\,^2\Delta$), TiF^{3+} ($^1\Sigma^+$), ZrF^+ ($^3\Sigma^-$), ZrF^{2+} ($^2\Delta$), and ZrF^{3+} ($^1\Sigma^+$). Specifically, for the TiF^+, they report r_e=1.81 Å ($^3\Phi$) and 1.77 Å ($^3\Sigma^-$), D_e ($^3\Phi$)=5.6 eV, and T_e ($^3\Sigma^- \leftarrow {}^3\Phi$)=5.7 kcal/mol, implying that $^3\Phi$ is the ground state. It is fair to mention at this point that as early as 1968, Hastie and Margrave[6] reported a thermochemically obtained D_0 TiF^+ value of about 6.5 eV, as cited in Ref. 5 (but see below). In 1999 Focsa and Pinchemel[7] using dispersed laser-induced fluorescence spectroscopy extended their previous work on TiF^+, by observing two low-lying excited states tagged $B\,^3\Delta$ and $C\,^3\Pi$, located ~2040 and ~2200 cm^{-1} above the ground state. They also provided more accurate directly determined ω_e values for the $^3\Phi$ and $^3\Delta$ states, 762 and 860 cm^{-1}, respectively, as opposed to 781(6) and 880(8) cm^{-1} previously determined.[4]

On the CrF^+ ion now, the only experimental results are those of Kent and Margrave[8] limited to the ionization energy (IE) of the (neutral) CrF molecule, obtained by high temperature mass spectroscopy, IE=8.4±0.3 eV. This value, combined with the dissociation energy of CrF, D_0=106.4

a)Electronic mail: mavridis@chem.uoa.gr

± 3.5 kcal/mol determined in the same work, allows for the "indirect" determination of the CrF^+ D_0 value through the expression

$$D_0(\mathrm{CrF}) - D_0(\mathrm{CrF}^+) = \mathrm{IE}_0(\mathrm{CrF}) - \mathrm{IE}(\mathrm{Cr}), \quad (1)$$

or $D_0(CrF^+) = 106.4 \pm 3.5$ kcal/mol $+ 6.76$ eV (Ref. 9) $- 8.4 \pm 0.3$ eV (Ref. 8) $= 68.6 \pm 10.4$ kcal/mol, a rather low estimate by about 15 kcal/mol, disregarding the uncertainty of 10 kcal/mol (*vide infra*). We remind that for a diatomic species MX and its cation MX^+ dissociating into $M^+ + X$, Eq. (1) holds under the proviso that, asymptotically, X should be in the same state for both reactions $MX \rightarrow M + X$ and $MX^+ \rightarrow M^+ + X$, and M, M^+ should be in their ground states.

Almost two decades later Harrison published *ab initio* calculations on CrF^+ based on configuration interaction (CI) methods with modest size basis sets (CISD/$[5s4p3d/_{Cr}4s3p1d/_F]$).[10] The ground state was found to be of $^5\Sigma^+$ symmetry with D_e, r_e, and ω_e values of 73.2 kcal/mol, 1.755 Å, and 769 cm^{-1}, respectively. However, it is worth noting that Harrison suspected that the experimental dissociation energy of 69 kcal/mol obtained using the results of Kent and Margrave[8] was rather low, so he proposed that a more "realistic" D_e value should be close to 90 kcal/mol, which is, indeed, the case (*vide infra*). In this work a $^5\Pi$ state is also reported with a $D_e = 72.6$ kcal/mol and $r_e = 1.773$ Å, 14 kcal/mol above the $X\,^5\Sigma^+$ state.

As far as we know, no experimental or theoretical results of any kind exist in the literature on the MF^- anions.

We herein report high level *ab initio* quantum mechanical calculations based on multireference configuration interaction (MRCI) and coupled-cluster (CC) methods combined with large to very large basis sets. For the cationic MF^+ series we calculated 3, 4, 5, 10, and 7 electronic states for the ScF^+, TiF^+, VF^+, CrF^+, and MnF^+, respectively, using both the MRCI and for certain states the CC methodology. For the anionic MF^- sequence the CC approach was used exclusively; we calculated the ground and some low-lying excited states. Finally, for reasons of completeness, we have also examined the $X\,^1\Sigma^+$ and the $a\,^3\Delta$ states of the neutral ScF molecule which had not been investigated in Ref. 1.

For all $MF^{\pm}$ and ScF species and states studied, we present full potential energy curves, binding energies, charge distributions, and the usual spectroscopic constants (r_e, ω_e, $\omega_e x_e$, α_e), trying at the same time to rationalize the bonding mechanisms. We believe that this work, combined with our previous investigation of the neutral MFs (M = Ti, V, Cr, and Mn),[1] will be of considerable help in understanding the electronic structure of the transition metal monohalides, and that will serve as a ground zero for future work on relevant polyatomic systems by experimentalists and theoreticians alike.

The paper is structured as follows: In Sec. II we outline some technical details and in Sec. III we summarize results pertaining to the neutral MFs, M = Sc to Mn. Two sections IV A and IV B, present our findings on the MF^+ and MF^- series, while a synopsis and some final remarks are given in Sec. V.

II. COMPUTATIONAL METHODS

In order of our results to be directly comparable with those of the corresponding neutral fluorides,[1] the same basis sets and methods were used in the present work. For the Sc, Ti and for V, Cr, and Mn metal atoms the atomic natural orbital (ANO) Gaussian basis sets of Bauschlicher[11] $21s16p9d6f4g$ and $20s15p10d6f4g$, respectively, were employed. For the F atom Dunning's[12] correlation consistent basis set of quadruple-ζ quality augmented with a single series of diffuse functions, $13s7p4d3f2g$ (aug-cc-pVQZ $\equiv$AQZ), was used. Both sets were generally contracted to $[7s6p4d3f2g/_M 6s5p4d3f2g/_F]$ engendering to a one-electron space of 164 spherical Gaussian functions. This basis set was used uniformly for the construction of complete potential energy curves (PEC) for the whole $MF^{\pm}$ series and states, as well as for two PECs of the neutral ScF molecule. For the TiF^+ cation only, the relatively recently developed Ti correlation consistent-type basis sets of Bauschlicher of quadruple (QZ$\equiv 7s8p6d3f2g1h$) and quintuple (5Z $\equiv 7s8p6d4f3g2h1i$) quality,[13] were also tested on all four TiF^+ states presently studied. Fluorine's accompanying bases are those of Dunning,[12] AQZ and A5Z, respectively. Moreover, in the core-valence calculations (*vide infra*), the Ti QZ and 5Z bases were further augmented by $1g1h$ (CQZ) and $1f1g1h$ (C5Z) sets of core Gaussian functions. Thus, our largest one-electron space used for the TiF^+ system, $[7s8p6d5f4g3h1i/_{Ti}7s6p5d4f3g2h/_F]$, consists of 305 spherical Gaussian functions.

The complete active space self-consistent field (CASSCF) + single + double excitations (CASSCF + 1 + 2 = MRCI/$_{ANO/AQZ}$) approach was employed for the calculation of all the PECs. Our valence space for the MF^+ systems consists of seven orbital functions correlating asymptotically to M^+ $(4s3d) + F(2p_z)$; note that the $2s2p_x2p_y$ F orbitals were not included in the active space. In the neutral ScF molecule the active space was extended by a $4p_z$ (Sc) orbital, thus containing eight orbital functions. The zeroth-order space is constructed by allotting four (ScF), three (ScF^+), four (TiF^+), five (VF^+), six (CrF^+), and seven (MnF^+) electrons among eight (ScF) and seven (MF^+) orbital functions giving rise to 65, 34, 55, 60, 35, and 18 configuration functions (CF), respectively, and according to space-spin symmetries. All calculations were done under C_{2v} symmetry constraints but CASSCF expansions obey correct axial ($|\Lambda|$) symmetries.

Additional (dynamical) valence correlation was taken into account by single and double excitations out of the CASSCF wave functions keeping the $1s2s2p3s3p/_M$ $1s/_F$ core orbitals doubly occupied, applying at the same time the internally contracted technique as implemented in the MOLPRO 2002.6 package.[14] The ground state ic-MRCI expansions range from about 445 000 ($ScF/X\,^1\Sigma^+$) to 1 000 000 CFs ($VF^+/X\,^4\Pi$). The corresponding TiF^+ ic-MRCI expansion within the extended $5Z/_{Ti}$ $A5Z/_F$ basis comprises 1.8×10^6 CFs.

Core-valence correlation was estimated by allowing single and double replacements out of the $3s^23p^6$ e^- of the M atoms in the CI procedure. These calculations will be referred to as C-MRCI. The internally contracted C-MRCI

expansions increase considerably, ranging from 1.3×10^6 (ScF/$X\,^1\Sigma^+$) to 3.3×10^6 CFs ($VF^+/X\,^4\Pi$) to 6.4×10^6 CFs ($TiF^+/X\,^3\Phi$), using the C5Z/A5Z one-electron basis.

For the entire MF^+ series and for certain states, ground states included, we also performed coupled cluster+singles +doubles including perturbative connected triples using restricted Hartree–Fock orbitals [RCCSD(T)]. These calculations were limited around equilibrium interatomic distances. RCCSD(T) calculations including excitations out of the $3s^23p^6$ semicore M^+ electrons will be referred to as C-RCCSD(T).

Now for the anionic series MF^-, $M=$ Sc, Ti, V, Cr, and Mn complete potential curves for all states considered were calculated at the RCCSD(T)/[ANO/$_M$AQZ/$_F$] level of theory, while C-RCCSD(T)/[ANO/$_M$AQZ/$_F$] calculations of the same states were also performed around equilibrium. Certain calculations on the MF^- species were done with the ACESII program.[15]

Scalar relativistic effects for all species studied and practically for all states, were estimated at both the MRCI and C-MRCI levels through the one-electron first-order Douglas-Kroll (DK) approximation,[16] while keeping the ANO (M^+) and AQZ (F) basis sets uncontracted.

One of the most serious drawbacks of the MRCISD approach is the lack of size extensivity, particularly influencing dissociation energies. Size nonextensivity errors at the [MRCI($+Q$), C-MRCI($+Q$)] level are [1.03 (0.26), 21.1 (3.8); 1.9 (0.1), 21.9 (4.0); 12.9 (3.6), 29.6 (4.7); 15.8 (4.3), 31.4 (5.0); 7.5 (1.1), 24.7 (4.7)] $m\mathrm{E_h}$ for the ScF^+, TiF^+, VF^+, CrF^+, and MnF^+ ground states, respectively. Employing the multireference averaged coupled pair functional (MRACPF) formulation[17] for the valence electrons, it is found that size nonextensivity errors are comparable with those of the $+Q$ (=Davidson) correction, being -0.28, -0.6, 3.3, 2.4, and -0.2 $m\mathrm{E_h}$ for the MF^+ sequence of ground states.

Finally, two more points should be mentioned. (a) The state-averaged[18] approach was used for most of the states of the MF^+ systems for purely technical reasons, and (b) basis set superposition errors (BSSE) were not considered because they are indeed negligible as compared to all other approximations made in the present work; for the dissociation energies of neutral MFs and using the same basis sets, BSSEs do not exceed 0.4 kcal/mol.[1]

III. THE NEUTRAL *M*Fs, *M*=Sc TO Mn

In Ref. 1 we examined the neutral fluorides TiF, VF, CrF, and MnF. Here, and for reasons of continuity and/or completeness, we present results for two states of the ScF system, namely the ground ($X\,^1\Sigma^+$) and the first excited ($a\,^3\Delta$) state, Table I. A very brief summary of the most important findings on the ground states of all five MFs including relevant experimental results, is given in Table II.

ScF. What is known experimentally on the $X\,^1\Sigma^+$ and $a\,^3\Delta$ states of ScF in connection to the present calculations, can be condensed as follows:

(1) $X\,^1\Sigma^+$: Thermochemically obtained dissociation energy, $D_0=140.8\pm3$ (Ref. 19) and 143.2 ± 3.2 kcal/mol,[20] $r_e=1.787$ Å, $\omega_e/\omega_e x_e=735.0/3.604\ \mathrm{cm^{-1}}$, and $\alpha_e=2.638\times10^{-3}\mathrm{cm^{-1}}$ from laser-induced fluorescence spectroscopy;[21] permanent dipole moment $\mu=1.72(2)$ Debye from Stark shift measurements.[22]

(2) $a\,^3\Delta$: $r_e=1.860$ Å, $\omega_e/\omega_e x_e=649.3/3.17\ \mathrm{cm^{-1}}$, $\alpha_e=2.58\times10^{-3}\ \mathrm{cm^{-1}}$, and $T_0(a\,^3\Delta\leftarrow X\,^1\Sigma^+)=1969.0\ \mathrm{cm^{-1}}$, from rotational spectroscopy.[23]

In 1967 Carlson and Moser calculated for the first time the $^1\Sigma^+$ and $^3\Delta$ states of ScF at the Hartree–Fock level, estimating semiempirically the effect of differential correlation between the two states.[24] They suggested that the $^1\Sigma^+$ state is lower than the $^3\Delta$ by just 461 $\mathrm{cm^{-1}}$. The first "modern" work on ScF is that by Harrison, who 20 years ago studied 30 states at low resolution by the generalized valence bond (GVB) and valence CISD/($5s4p3d/3s3p1d$) methods.[25] He found that $^1\Sigma^+$ is the ground state with a $^3\Delta$ 2420–4840 $\mathrm{cm^{-1}}$ higher, and $D_0(X\,^1\Sigma^+)=100$ kcal/mol at the GVB level.

In 1988 Langhoff *et al.*[26] studied the ScX and YX halides, $X=$ F, Cl, and Br using MRCI and coupled pair functional [CPF (Ref. 27)] methods. In particular, for the ScF molecule they calculated 17 states using a [$8s6p4d3f/_{Sc}4s4p2d1f/_F$] basis, taking also into account Darwin and mass velocity relativistic effects through first-order perturbation theory. The ground state was found to be of $^1\Sigma^+$ symmetry with the $a\,^3\Delta$-$X\,^1\Sigma^+$ splitting ranging from 612 $\mathrm{cm^{-1}}$ (valence-MRCI) to 2780 $\mathrm{cm^{-1}}$ (core-CPF +relativity). Their best CPF D_0, r_e, and μ values for the X state are 138.4 kcal/mol, 1.790 Å, and 1.721 D, respectively, in excellent agreement with the experimental results.

Finally, Chrissanthopoulos and Maroulis,[35] with the purpose of obtaining accurate dipole moment and polarizability values of the $X\,^1\Sigma^+$ state of ScF, they used three basis sets of increasing size. Their best μ value at the CCSD(T)/[$7s5p5d3f/6s4p4d2f$] level is 1.500 D, 0.22 D smaller than the experimental one.

Table I lists our numerical findings on the $X\,^1\Sigma^+$ and $a\,^3\Delta$ states of ScF, while Fig. 1 shows the corresponding potential energy curves. The main CASSCF equilibrium CFs and Mulliken atomic distributions (Sc/F) of these two states are

$$|X\,^1\Sigma^+\rangle\cong0.95|(\mathrm{core})^{20}1\sigma^2 2\sigma^2 3\sigma^2 1\pi_x^2 1\pi_y^2\rangle 4s^{1.52}4p_z^{0.17}4p_{x,y}^{0.12}3d_{z^2}^{0.37}3d_{xz}^{0.06}3d_{yz}^{0.06} 3d_{x^2-y^2}^{0.01}3d_{xy}^{0.01}/2s^{1.96}2p_z^{1.81}2p_x^{1.93}2p_y^{1.93},$$

$$|a\,^3\Delta\rangle\cong0.997|(\mathrm{core})^{20}1\sigma^2 2\sigma^2 3\sigma^1 1\pi_x^2 1\pi_y^2 1\delta_+^1\rangle 4s^{0.84}4p_z^{0.18}3d_{z^2}^{0.12}3d_{xz}^{0.04}3d_{yz}^{0.04}3d_{x^2-y^2}^{1.0} 3d_{xy}^{0.04}/2s^{1.98}2p_z^{1.86}2p_x^{1.94}2p_y^{1.94},$$

where the orbital numbering refers to valence electrons only and $(\mathrm{core})^{20}\equiv1s^22s^22p^63s^23p^6(\mathrm{Sc})+1s^2(\mathrm{F})$.

About $0.65e^-$ and $0.70e^-$ are transferred from Sc to the $2p_z$ orbital of F in the $X\,^1\Sigma^+$ and $a\,^3\Delta$ states, therefore the *in situ* description is $Sc^+(3d^14s^1;\,^1D)-F^-$ and $Sc^+(3d^14s^1;\,^3D)-F^-$, respectively. Adiabatically both states correlate to $Sc(^2D)+F(^2P)$. Note, however, that we

TABLE I. Total energies E (hartree), bond distances r_e (Å), dissociation energies D_e (kcal/mol), harmonic and anharmonic frequencies ω_e, $\omega_e x_e$ (cm^{-1}), rotational-vibrational constants α_e (cm^{-1}) dipole moments μ (D), total charges on Sc q_{Sc}, and energy separations T_e (cm^{-1}) for the $X\,^1\Sigma^+$ and $a\,^3\Delta$ states of ScF.

Method	$-E$	r_e	D_e[a]	ω_e	$\omega_e x_e$	α_e	$\langle\mu\rangle/\mu_{FF}$[b]	q_{Sc}	T_e
				$X\,^1\Sigma^+$					
MRCI	859.637 13	1.824	137.2	733	4.5	0.002 7	1.38/1.61	0.64	0.0
MRCI+Q[c]	859.653 91	1.826	141.0	733	4.5	0.002 7			0.0
MRCI+DK[d]	863.275 44	1.827					1.37/1.55	0.79	0.0
MRCI+DK+Q[c,d]	863.292 07	1.829							0.0
C-MRCI[e]	859.881 67	1.792	134.8	727	3.6	0.002 7	1.23/1.70	0.62	0.0
C-MRCI+Q[c,e]	859.936 35	1.791	141.0	730	3.6	0.002 6			0.0
C-MRCI+DK[d,e]	863.561 88	1.791	135.4				1.21/1.68	0.79	0.0
C-MRCI+DK+Q[c,e]	863.620 02	1.790	140.8						0.0
RCCSD(T)	859.653 18	1.867	138.8	709	3.4	0.001 2	···/1.52		0.0
RCCSD(T)+DK[d]	863.292 01	1.865	141.0				···/1.42		0.0
C-RCCSD(T)[e]	859.951 46	1.789	144.6	735	2.6	0.002 7	···/1.70		0.0
C-RCCSD(T)+DK[d,e]	863.637 02	1.790	144.5				···/1.68		0.0
Expt.[f]		1.787	140.8±3[g] 143.2±3.2[g]	735	3.604	0.002 64	1.72(2)		
				$a\,^3\Delta$					
MRCI	859.628 06	1.899	131.5	629	3.2	0.002 7	2.53/2.77	0.70	1990
MRCI+Q[c]	859.643 82	1.899	134.7	628	3.2	0.002 8			2213
MRCI+DK[d]	863.261 26	1.897					2.52/2.80	0.89	3113
MRCI+DK+Q[c,d]	863.277 14	1.897							3277
C-MRCI[e]	859.876 05	1.868	131.2	641	2.8	0.002 4	2.39/2.82	0.71	1233
C-MRCI+Q[c,e]	859.928 93	1.863	136.3	644	2.9	0.002 5			1628
C-MRCI+DK[d,e]	863.551 55	1.868	128.9				2.40/2.85	0.89	2269
C-MRCI+DK+Q[c,e]	863.608 42	1.864	133.5						2545
RCCSD(T)	859.639 40	1.990	130.2	608	5.1	0.001 7	···/2.80		3023
C-RCCSD(T)[e]	859.943 02	1.861	139.3	646	3.0	0.002 5	···/2.92		1853
C-RCCSD(T)+DK[d,e]	863.624 56	1.862	136.7				···/2.95		2735
Expt.[f]		1.860		649.3	3.17	0.002 58			1969.0

[a]With respect to ground state fragments Sc (^2D)+F (^2P).
[b]$\langle\mu\rangle$ calculated as expectation value, μ_{FF} by the finite field method.
[c]+Q, the Davidson correction.
[d]DK, Douglas–Kroll relativistic corrections.
[e]The "core" $3s^2 3p^6$ electrons of Sc have been included.
[f]See text.
[g]D_0.

were unable to calculate the adiabatic potential energy curves; the PECs shown in Fig. 1 have *diabatic* character, i.e., respresent the dissociations Sc^+F^- ($X\,^1\Sigma^+, a\,^3\Delta$) $\rightarrow Sc^+(^1D, ^3D)+F^-(^1S)$. This is also clear from the energy separation between the two states at 8 Å which is 2573 (2428) cm^{-1} at the MRCI(+Q) level, in conformity with the experimental atomic splitting[9] $Sc^+(^3D \leftarrow ^1D) = 2407\ cm^{-1}$.

From Table I we can see that at the highest level of calculation, C-MRCI+DK+Q or C-RCCSD(T)+DK, the calculated bond distance of the $X\,^1\Sigma^+$ state is in excellent agreement with experiment, 1.790 versus 1.787 Å. The same holds true for D_e; the most recent experimental value[20] is in complete agreement with the C-RCCSD(T) result, while the C-MRCI+DK+Q D_e value falls short by 2.5 kcal/mol. The DK-relativistic corrections are practically negligible for r_e and D_e in both the C-MRCI and C-RCCSD(T) methods, but the D_e value increases by 2.2 kcal/mol at the RCCSD(T) level. For technical reasons it was not possible to calculate the adiabatic supermolecule at the MRCI+DK level, so we do not report the corresponding D_e value.

Concerning now the dipole moment of the $X\,^1\Sigma^+$ state, the general observation is that finite field values (μ_{FF}) are in good to excellent agreement with experiment[22] in both multireference and coupled-cluster methods, but this is not true for expectation values ($\langle\mu\rangle$) at the MRCI or C-MRCI level of theory; see also Ref. 36 for a discussion of $\langle\mu\rangle$ versus μ_{FF} values.

The first excited state is of $^3\Delta$ symmetry located 1969.0 cm^{-1} higher according to the experimental findings of Shenyavskaya *et al.*,[23] reflecting the *in situ* Sc^+ ($^3D \leftarrow ^1D$) splitting[9] of 2407 cm^{-1}. MRCI and C-RCCSD(T) $T_e(a\,^3\Delta \leftarrow X\,^1\Sigma^+)$ results are in very good agreement with experiment, while the C-MRCI+Q value can only be considered as fair due to large size non-extensivity errors and the inherent uncertainties in the +Q Davidson correction. DK-relativistic corrections, of similar size in both multireference and coupled-cluster approaches, increase the T_e values by about 1000 cm^{-1}. At the highest level of calculation C-MRCI+DK+Q and C-RCCSD(T)+DK, we obtain $T_e = 2545$ and 2735 cm^{-1}, respectively. These fluctuating T_e values upon gradually increasing the size of calculation but not necessarily the "quality" of the wave function, indicate

TABLE II. Dissociation energies D_e (kcal/mol), bond distances r_e (Å), harmonic frequencies ω_e (cm^{-1}), and dipole moments μ (D) of the ground state neutral fluorides ScF ($X\,^1\Sigma^+$), TiF ($X\,^4\Phi$), VF ($X\,^5\Pi$), CrF ($X\,^6\Sigma^+$), and MnF ($X\,^7\Sigma^+$). Experimental values in parenthesis.

Species	D_e[c]	r_e[d]	ω_e[e]	μ[f]
ScF[a]	144	1.790	727	1.70/1.70
	(140.8±3)[g,h]	(1.787)[j]	(735.0)[j]	[1.72(2)][k]
	(143.2±3.2)[g,i]			
TiF[b]	135	1.839	655	2.95/2.80
	(136.0±8)[g,l]	(1.8311)[m]	(650.7)[m,n]	
VF[b]	130	1.788	652	2.82/3.25
		(1.7758)[o]	(670.7)[o]	
CrF[b]	110	1.785	666	4.27/4.22
	(106.4±3.5)[g,p]	(1.7839)[q]	(664)[q]	
MnF[b]	108	1.840	623	2.90/2.75
	(104.5±2.3)[g,r]	(1.8387)[t]	(624.2)[t]	
	(106.4±1.8)[g,s]			

[a]Present work.
[b]Values from Ref. 1.
[c]With respect to ground state atoms; best estimates, see Ref. 1.
[d]RCCSD(T) values including the $3s^23p^6$ electrons of the metal atom [C-RCCSD(T)].
[e]MRCI values including the $3s^23p^6$ electrons of the metal atom (C-MRCI).
[f]Finite field values at the C-MRCI/C-RCCSD(T) level.
[g]D_0 values.
[h]Reference 19.
[i]Reference 20.
[j]Reference 21.
[k]Reference 22.
[l]Reference 28.
[m]Reference 29.
[n]$\Delta G_{1/2}=\omega_e-2\omega_e x_e$.
[o]Reference 30.
[p]Reference 8.
[q]Reference 31.
[r]Reference 32.
[s]Reference 33.
[t]Reference 34.

clearly the difficulties of obtaining reliable results on these systems.

Concerning the bond distance, the usual convergence to the experimental value is observed as we move from the MRCI to C-MRCI to C-MRCI+DK to C-MRCI+DK+Q, the final value being 1.864 Å, or 1.862 Å at the C-RCCSD(T)+DK level, in excellent agreement with the experimental result.

Finally, the same observations can be made as before contrasting $\langle\mu\rangle$ versus μ_{FF} dipole moments. Our best estimate for the dipole moment on the $a\,^3\Delta$ state of ScF is 2.90±0.05 D; see Table I.

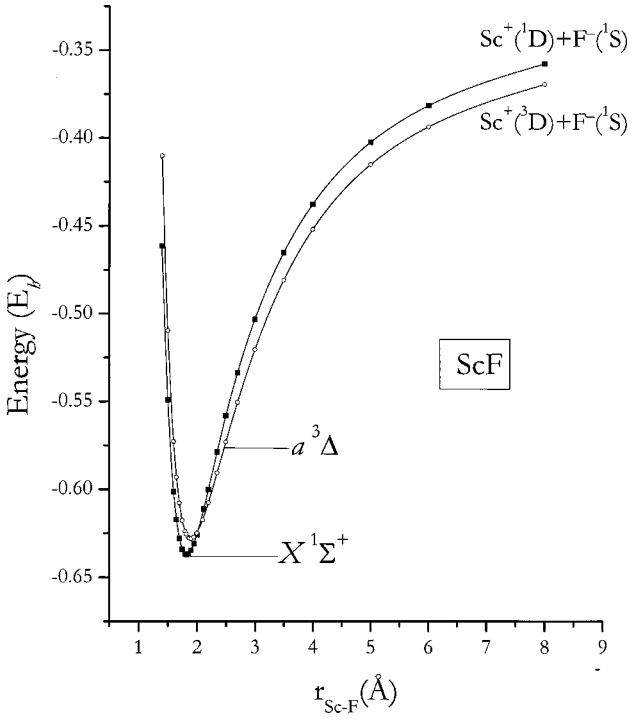

FIG. 1. MRCI/(ANO/AQZ) potential energy curves of $X\,^1\Sigma^+$ and $a\,^3\Delta$ states of ScF. See text. Energies shifted by $+859E_h$.

IV. RESULTS AND DISCUSSION

In what follows we first discuss the electronic structure of MF^+ species followed by the MF^- anions, M=Sc, Ti, V, Cr, and Mn.

A. The cations MF^+

The IEs of Sc, Ti, V, Cr, and Mn atoms are 6.561, 6.828, 6.746, 6.766, and 7.434 eV, respectively, while that of the F atom is 17.42 eV.[9] Therefore it is clear that all MF^+ cations dissociate adiabatically to $M^+ + F$. An altenative dissociative channel could be $M^{2+} + F^-$, but this channel is ruled out immediately because it is higher than the $M^+ + F$ channel by $\Delta E = IE(M^+) - EA(F) = IE(M^+) - 3.40$ eV (Ref. 37) =9.49, 10.23, 10.80, 13.09, 12.24 eV, for $M=Sc^+$, Ti^+, V^+, Cr^+, and Mn^+, respectively. Neverthelss, our calculations clearly indicate (*vide infra*) that at the equilibrium the *in situ* atoms can be described adequately as $M^{2+}F^-$, or that the MF^+ charged species are ionic. For all MF^+ systems and for all states studied the CASSCF and/or MRCI Mulliken populations indicate a charge transfer of $0.60e^- - 0.65e^-$ from M^+ to F, about $0.1e^-$ less than in the corresponding neutral fluorides. Hence, it is rather conceptually simpler to

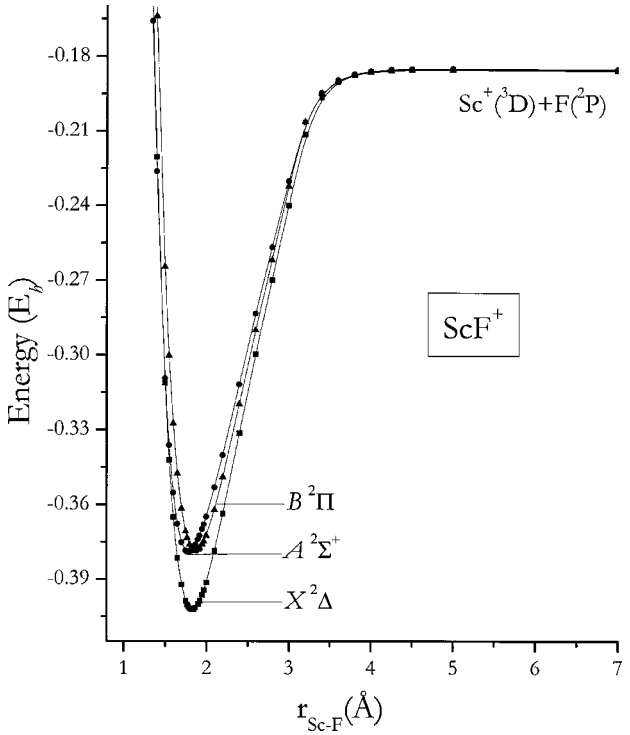

FIG. 2. MRCI PECs of $X\,^2\Delta$, $A\,^2\Sigma^+$, and $B\,^2\Pi$ states of ScF^+. Energies shifted by $+859E_h$.

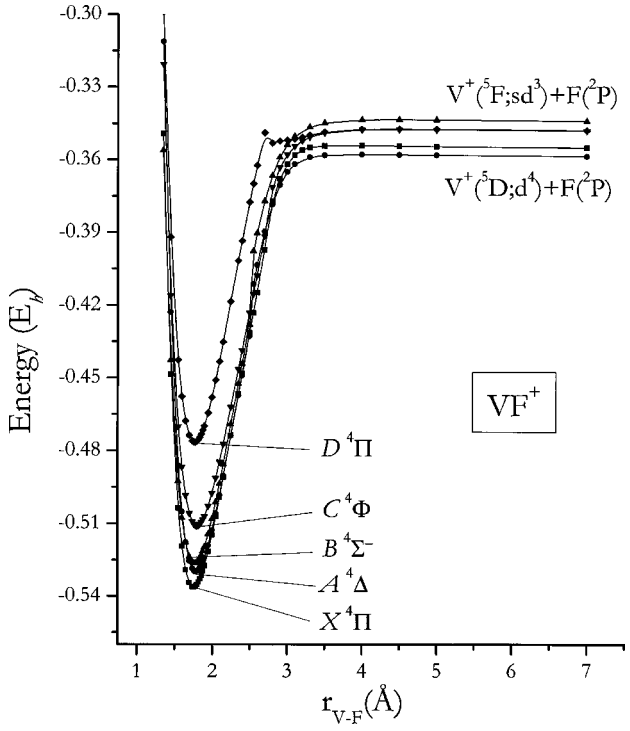

FIG. 4. MRCI PECs of $X\,^4\Pi$, $A\,^4\Delta$, $B\,^4\Sigma^-$, $C\,^4\Phi$, and $D\,^4\Pi$ states of VF^+. Energies shifted by $+1042E_h$.

consider that the MF^+ cations are formed from the corresponding MFs by removing one "nonbonding" $4s$ or $3d$ metal electron.

All our numerical results on MF^+s are presented in Tables III–VIII; Table IX lists the leading CASSCF CFs and atomic Mulliken equilibrium populations for every MF^+ state, while Figs. 2–6 show potential energy curves at the MRCI/(ANO/AQZ) level of theory. Because of the highly ionic character of the MF^+s and following the notation of Ref. 1, their equilibrium configurational description in Table

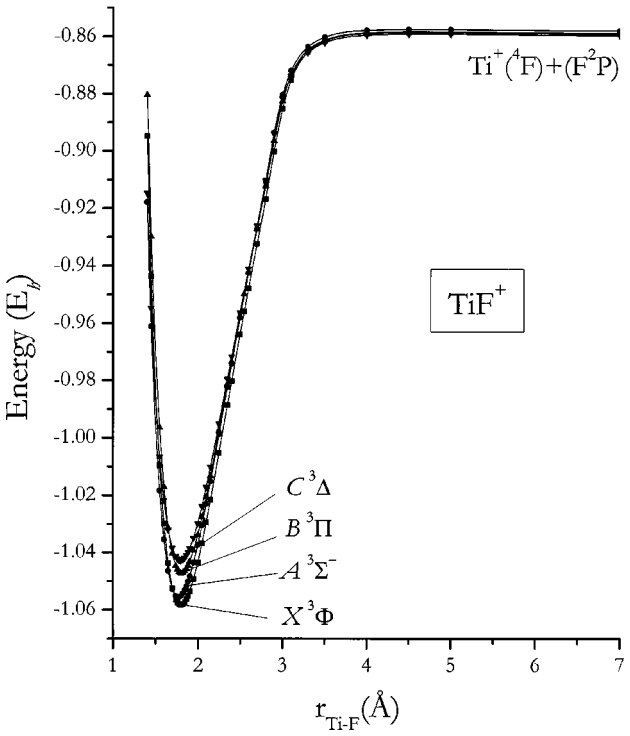

FIG. 3. MRCI PECs of $X\,^3\Phi$, $A\,^3\Sigma^-$, $B\,^3\Pi$, and $C\,^3\Delta$ states of TiF^+. Energies shifted by $+947E_h$.

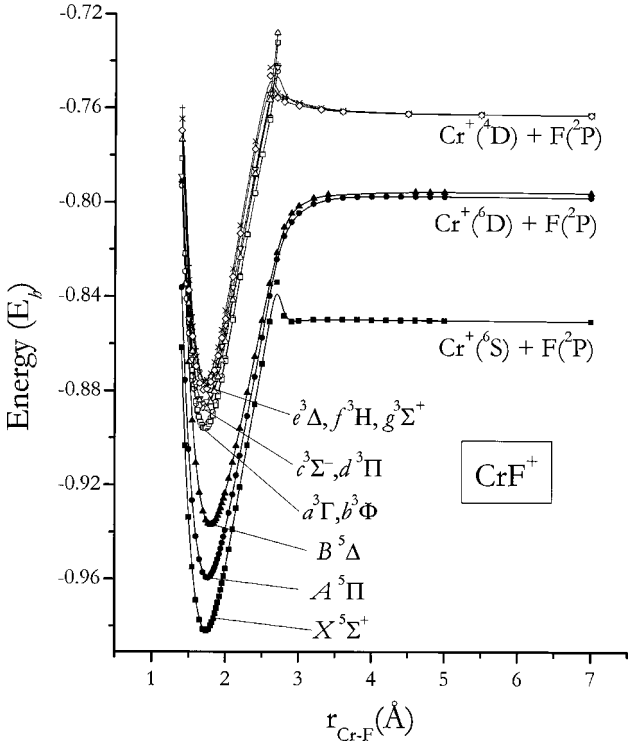

FIG. 5. MRCI PECs of $X\,^5\Sigma^+$, $A\,^5\Pi$, $B\,^5\Delta$, $a\,^3\Gamma$, $b\,^3\Phi$, $c\,^3\Sigma^-$, $d\,^3\Pi$, $e\,^3\Delta$, $f\,^3H$, and $g\,^3\Sigma^+$ states of CrF^+. Energies shifted by $+1142E_h$.

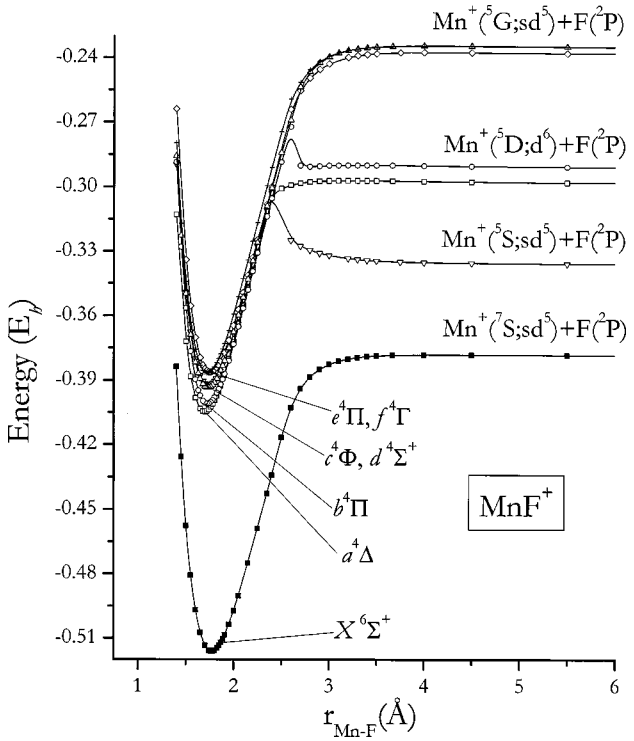

FIG. 6. MRCI PECs of $X\,^6\Sigma^+$, $a\,^4\Delta$, $b\,^4\Pi(1)$, $c\,^4\Phi$, $d\,^4\Sigma^+$, $e\,^4\Pi(2)$, and $f\,^4\Gamma$ states of MnF^+. Energies shifted by $+1249E_h$.

IX is limited to the valence space of the doubly charged *in situ* M^{2+} metal cations. An example will clarify what we mean. The leading ground state CASSCF configuration of ScF^+ is

$$|X\,^2\Delta\rangle = 0.997|(\text{core})^{20}1\sigma^2 2\sigma^2 1\pi_x^2 1\pi_y^2 1\delta_+^1\rangle,$$

where $(\text{core})^{20}$ represents the $1s^2 2s^2 2p^6 3s^2 3p^6 + 1s^2\ e^-$ of Sc and F. Note that the numbering of the orbitals refers to the valence electrons. Omitting from now on the common factor $(\text{core})^{20}1\sigma^2 2\sigma^2 1\pi_x^2 1\pi_y^2$ for all MF^+s, where the $1\sigma^2, 2\sigma^2, 1\pi_x^2, 1\pi_y^2$ reflect the $2s^2, 2p_z^2, 2p_x^2, 2p_y^2$ atomic orbitals of F^-, the above CASSCF configuration of the $X\,^2\Delta$ state of ScF^+ is condensed to $0.997|1\delta_+^1\rangle$; see Table IX.

1. ScF^+

No experimental or theoretical results of any kind exist in the literature on ScF^+. The CASSCF (and MRCI) Mulliken equilibrium distributions suggest, as in all MF^+ species studied here, that about $0.65e^-$ are transferred to the F from the Sc^+ cation (Table IX). The symmetry of the resulting states $^2\Sigma^+$, $^2\Pi$, and $^2\Delta$ is dictated by the single $3d$ electron of Sc^{2+} $(3d^1; {}^2D)$ in the field of F^-. Table III proves and Fig. 2 shows that the ground state of ScF^+ is of $^2\Delta$ symmetry with two close-lying states of $^2\Sigma^+$ and $^2\Pi$ symmetries. At the highest multireference level, C-MRCI + relativistic corrections + Davidson correction = C-MRCI + DK + Q, we predict a binding energy $D_e(X\,^2\Delta) = 137.2$ kcal/mol at $r_e = 1.796$ Å. Recalling that we are dealing with a single reference system our coupled-cluster results should be very reliable. Assuming approximate additivity of DK-relativistic effects at the multireference and CC level (as the CrF^+ case suggests, see below) which are -1.4 and -3.1 kcal/mol at the MRCI + DK − MRCI, C-MRCI + DK − (C-MRCI), respectively, we obtain D_e[RCCSD(T)] $= 135.5 - 1.4 = 134.1$ kcal/mol, and D_e[C-RCCSD(T)] $= 143.3 - 3.1 = 140.2$ kcal/mol at $r_e = 1.795$ Å. Note that the RCCSD(T) approach, i.e., without the $3s^2 3p^6$ electrons, fails in predicting a reasonable bond distance even in comparison with the MRCI wave function.

Taking also into account our C-MRCI + Q results we suggest that $D_e(X\,^2\Delta) = 140$ kcal/mol and $r_e = 1.795$ Å.

The next two states, $^2\Sigma^+$ and $^2\Pi$, are practically degenerate at the MRCI level; see Table III and Fig. 2. However, by improving the quality of calculation the two states split apart by more than 2000 cm^{-1}, the $^2\Sigma^+$ becoming the first excited state. Indeed, at the highest multireference level, C-MRCI + DK + Q, $\Delta E(^2\Pi \leftarrow {}^2\Sigma^+) = 2443$ or 2045 cm^{-1} at the C-RCCSD(T) level. Including the relativistic effects as obtained from the C-MRCI, (C-MRCI + DK) to the C-RCCSD(T) results, the above difference becomes 2908 cm^{-1}. Therefore it is certain that the ordering of states is $X\,^2\Delta$, $A\,^2\Sigma^+$ and $B\,^2\Pi$ with $A\,^2\Sigma^+ - X\,^2\Delta$, $B\,^2\Pi - X\,^2\Delta$ separations of about 3000 and 5500 cm^{-1}, respectively.

2. TiF^+

As described in the introduction only recently Focsa *et al.*[4,7] determined the bond distance $r_e = 1.7800(1)$ Å and harmonic frequency $\omega_e = 760$ cm^{-1} of the $^3\Phi$ state of TiF^+, suggesting also that the ground state is of $^3\Phi$ symmetry. In addition, Focsa and Pinchemel[7] determined two very close low-lying states, named, $B\,^3\Delta$ and $C\,^3\Pi$, located ~ 2040 and ~ 2200 cm^{-1} above the $^3\Phi$ state; see Table IV.

The only theoretical results on TiF^+ are those of Schröder *et al.*,[5] who at the RCCSD(T) level predict as well that $^3\Phi$ is the ground state with a $^3\Sigma^-$ state 5.7 kcal/mol higher and a binding energy of 129 kcal/mol (see Sec. I).

As in all five MF^+ species studied here the TiF^+ cation is highly ionic, its equilibrium being described accurately enough as $Ti^{2+}F^-$. Because the Ti^{2+} ground term is ^3F $(3d^2)$, four close-lying molecular triplets of symmetries Σ^-, Π, Δ, and Φ are expected. This is indeed what we find; see Fig. 3.

First, a general observation: Our results for the four triplets above are very similar in the two basis sets used, Tables IV and V. For the $^3\Phi$ state at the highest level of multireference calculation C-MRCI + DK + Q [C-MRCI + DK + Q/(C5Z/A5Z)], the binding energy with respect to the ground state fragments is predicted to be 125.7 [126.6] kcal/mol, a difference of just +0.9 kcal/mol in moving from the $[7s6p4d3f2g/_{Ti} 6s5p4d3f2g/_F]$ to $[7s8p6d5f4g3h1i/_{Ti}\ 7s6p5d4f3g2h/_F]$, where the one-electron space is almost doubled. Corresponding C-RCCSD(T) [C-RCCSD(T)/(C5Z/A5Z)] results are 132.0 [132.4] kcal/mol. Assuming as before additivity of DK effects as obtained from the C-MRCI results, the CC D_e value reduces to 128.2 [129.8] kcal/mol. Therefore, our recommended D_e value for the $^3\Phi$ state of TiF^+ is 130 kcal/mol. The calculated r_e values at both C-MRCI + DK and C-RCCSD(T) level are in excellent agreement with the experimental number.[4] The same holds

TABLE III. Results on the $X\ ^1\Sigma^+$, $A\ ^2\Sigma^+$, and $B\ ^2\Pi$ states of ScF^+. Symbols, units, and acronyms as in Table I.

Method	$-E$	r_e	D_e	ω_e	$\omega_e x_e$	α_e	q_{Sc}	T_e
			$X\ ^2\Delta$					
MRCI	859.402 27	1.829	136.0	732	3.0	0.0023	1.59	0.0
MRCI+Q	859.417 23	1.831	139.5	731	3.1	0.0022		0.0
MRACPF	859.414 38	1.832	138.8	724	2.3	0.0022	1.55	0.0
MRCI+DK	863.033 69	1.828	134.6	728	2.6	0.0022	1.78	0.0
MRCI+DK+Q	863.048 71	1.830	138.0	729	3.2	0.0023		0.0
C-MRCI	859.647 36	1.798	135.1	746	2.8	0.0023	1.58	0.0
C-MRCI+Q	859.698 34	1.795	140.3	747	2.7	0.0022		0.0
C-MRCI+DK	863.320 96	1.798	132.0	746	2.9	0.0022	1.79	0.0
C-MRCI+DK+Q	863.375 78	1.796	137.2	747	2.9	0.0022		0.0
RCCSD(T)	859.414 02	1.891	135.5	697	2.8	0.0006		0.0
C-RCCSD(T)	859.710 65	1.795	143.3	748	2.9	0.0023		0.0
			$A\ ^2\Sigma^+$					
MRCI	859.379 05	1.783	121.7	721	6.2	0.0040	1.53	5097
MRCI+Q	859.397 19	1.780	127.1	743	6.8	0.0038		4399
MRACPF	859.394 85	1.782	126.8	736	5.4	0.0036	1.44	4286
MRCI+DK	863.015 63	1.774	123.5	761	6.6	0.0035	1.69	3965
MRCI+DK+Q	863.033 88	1.774	129.0	776	6.5	0.0033		3255
C-MRCI	859.624 35	1.756	120.7	741	5.5	0.0036	1.54	5050
C-MRCI+Q	859.679 98	1.748	128.7	774	5.7	0.0033		4030
C-MRCI+DK	863.301 79	1.751	120.1	763	5.2	0.0033	1.72	4206
C-MRCI+DK+Q	863.361 46	1.746	128.2	791	5.0	0.0029		3142
RCCSD(T)	859.396 98	1.814	124.8	736	8.4	0.0027		3739
C-RCCSD(T)	859.693 80	1.753	132.7	770	3.4	0.0028		3698
			$B\ ^2\Pi$					
MRCI	859.378 52	1.871	121.0	692	2.4	0.0023	1.64	5211
MRCI+Q	859.394 05	1.873	124.8	690	2.4	0.0023		5087
MRACPF	859.390 21	1.873	123.5	689	2.7	0.0024	1.62	5305
MRCI+DK	863.010 10	1.869	119.7	692	2.3	0.0023	1.78	5178
MRCI+DK+Q	863.025 69	1.871	123.5	690	2.5	0.0024		5052
C-MRCI	859.621 66	1.842	119.0	710	2.9	0.0022	1.64	5641
C-MRCI+Q	859.672 98	1.839	124.5	713	3.0	0.0022		5567
C-MRCI+DK	863.295 17	1.842	116.0	709	2.9	0.0022	1.80	5660
C-MRCI+DK+Q	863.350 33	1.839	121.4	713	3.1	0.0022		5585
RCCSD(T)	859.392 41	1.924	122.0	700	5.2	0.0012		4742
C-RCCSD(T)	859.684 48	1.840	126.9	710	2.9	0.0023		5743

true for the larger C5Z/A5Z basis set; see Table V. The agreement is also excellent between theory and experiment of the ω_e, $\omega_e x_e$, and α_e values, 760, 3.5, and 0.0023 cm^{-1}, respectively at the C-RCCSD(T) level as contrasted to the experimental ones 762, 3.4, and 0.0023 (Refs. 4 and 7).

We discussed first the $^3\Phi$ state only because it was the experimentalists' suggestion for the ground state of TiF^+.[4,7] However, our calculations indicate that a $^3\Sigma^-$ state competes strongly with the $^3\Phi$. Following the results of the $T_e(^3\Sigma^- \leftarrow ^3\Phi)$ energy separation at increasing level of calculation, we first note that these two states are degenerate within the accuracy of our approximations, Table IV. At the MRCI, MRCI+Q (or MRACPF), MRCI+DK, and MRCI+DK+Q, $^3\Phi$ remains the ground state, with the $^3\Sigma^-$ state about 500 cm^{-1} higher. Including the $3s^2 3p^6$ semicore electrons in the configuration interaction, the T_e reduces to about 200 cm^{-1}, and finally the order between the two states is inverted at the C-MRCI+Q and C-MRCI+DK+Q level by less than 100 cm^{-1}. Similarly, at the RCCSD(T) and C-RCCSD(T) level the ground state is of $^3\Sigma^-$ symmetry with the $^3\Phi$ higher by 72 and 850 cm^{-1}, respectively.

The above results follow the same pattern at the much larger basis set C5Z/A5Z, Table V. At this level the C-MRCI($+Q$) energy separation $T_e(^3\Sigma^- \leftarrow ^3\Phi) = 201(-61)$ cm^{-1} with the C-RCCSD(T) being -865 cm^{-1}.

It is obvious that within our methods we can not decide on the symmetry of the TiF^+ ground state; more accurate experimental (or theoretical) results are required to resolve this issue. Nevertheless it seems that the $^3\Sigma^-$ state is the stronger candidate of being the lowest state of TiF^+. The markings $X\ ^3\Phi$, $A\ ^3\Sigma^-$ given in Tables IV, V, and Fig. 3 are based on the MRCI, C-MRCI results and are only of formal significance. It should also be mentioned that the experimental estimate of Hastie and Margrave[6] (as cited in Ref. 5) of the dissociation energy, $D_0 \approx 150$ kcal/mol, is certainly overestimated by about 15 kcal/mol.

The next two states of TiF^+ present the same difficulty in deciding their relative order. According to experiment,[7] they are of $B\ ^3\Delta$ and $C\ ^3\Pi$ symmetry, about 2040 and 2200 cm^{-1} higher than the X state, $^3\Phi$. Our results are in practical agreement with the experimental findings but with a formal reversal of the $B\ ^3\Pi$ and $C\ ^3\Delta$ states. With respect to the $^3\Phi$ state our best $T_e(^3\Pi \leftarrow ^3\Phi)$ value at the C-MRCI+DK+Q level is 2219 cm^{-1}, differing by just 214 cm^{-1}

TABLE IV. Results on the $X\ ^3\Phi$, $A\ ^3\Sigma^-$, $B\ ^3\Pi$, and $C\ ^3\Delta$ states of TiF^+. Symbols, units, and acronyms as in Table I.

Method	$-E$	r_e	D_e	ω_e	$\omega_e x_e$	α_e	q_{Ti}	T_e
			$X\ ^3\Phi$					
MRCI	948.058 40	1.800	125.1	744	3.1	0.0023	1.65	0.0
MRCI+Q	948.076 15	1.800	129.6	744	3.2	0.0024		0.0
MRACPF	948.072 26	1.801	128.2	739	2.5	0.0023	1.62	0.0
MRCI+DK	952.477 75	1.798	123.3	743	3.0	0.0025	1.75	0.0
MRCI+DK+Q	952.495 56	1.797	127.8	743	3.0	0.0025		0.0
C-MRCI	948.327 64	1.780	123.2	757	2.9	0.0023	1.66	0.0
C-MRCI+Q	948.382 86	1.777	129.6	760	2.7	0.0024		0.0
C-MRCI+DK	952.792 76	1.780	119.4				1.76	0.0
C-MRCI+DK+Q	952.851 73	1.776	125.7					0.0
RCCSD(T)	948.076 61	1.814	128.6	741	3.6	0.0023		0.0
C-RCCSD(T)	948.389 20	1.779	132.0	760	3.5	0.0023		0.0
Expt.		1.7800[a]	150[b]	762[c]	3.4[c]	0.0023[c]		
			$A\ ^3\Sigma^-$					
MRCI	948.055 68	1.771	124.1	749	4.4	0.0028	1.62	597
MRCI+Q	948.073 80	1.768	128.9	741	3.1	0.0027		516
MRACPF	948.069 88	1.769	127.4	737	3.2	0.0027	1.60	522
MRCI+DK	952.475 24	1.768	122.5	745	3.6	0.0028	1.74	551
MRCI+DK+Q	952.493 46	1.766	127.2	746	3.4	0.0028		461
C-MRCI	948.326 75	1.750	122.8	757	3.5	0.0026	1.63	195
C-MRCI+Q	948.383 23	1.743	129.9	764	3.4	0.0026		−81
C-MRCI+DK	952.792 00	1.750	119.1				1.75	167
C-MRCI+DK+Q	952.852 16	1.743	126.1					−94
RCCSD(T)	948.076 94	1.778	128.8	752	3.6	0.0023		−72
C-RCCSD(T)	948.393 08	1.731	134.4	800	2.9	0.0024		−850
			$B\ ^3\Pi$					
MRCI	948.047 19	1.808	118.3	727	3.0	0.0024	1.65	2460
MRCI+Q	948.065 41	1.807	123.1	726	2.5	0.0024		2357
MRACPF	948.061 44	1.809	121.6	725	3.0	0.0023	1.62	2375
MRCI+DK	952.466 80	1.806	116.7	728	3.0	0.0023	1.75	2403
MRCI+DK+Q	952.485 09	1.805	121.4	729	3.0	0.0024		2298
C-MRCI	948.316 65	1.788	116.3	742	3.0	0.0023	1.66	2412
C-MRCI+Q	948.372 57	1.783	123.2	747	2.7	0.0023		2258
C-MRCI+DK	952.781 95	1.787	112.7					2373
C-MRCI+DK+Q	952.841 62	1.782	119.4					2219
Expt.[c]								~2200
			$C\ ^3\Delta$					
MRCI	948.042 83	1.797	115.1	668	2.0	0.0017	1.63	3417
MRCI+Q	948.062 60	1.788	120.8	660	0.3	0.0020		2974
MRACPF	948.057 98	1.794	119.0	665	0.9	0.0018	1.59	3134
MRCI+DK	952.464 63	1.782	114.8	663	0.3	0.0016	1.71	2880
MRCI+DK+Q	952.484 74	1.772	120.7	666	0.8	0.0022		2375
C-MRCI	948.311 36	1.774	112.9	681	2.7	0.0017	1.64	3573
C-MRCI+Q	948.369 37	1.758	121.1	684	3.8	0.0018		2961
C-MRCI+DK	952.778 92	1.761	110.6					3038
C-MRCI+DK+Q	952.841 12	1.743	119.0					2329
Expt.[c]								~2040

[a]Reference 4.
[b]Reference 6.
[c]Reference 7.

from the plain MRCI result, in agreement with the experimental separation. However, in the $^3\Delta$ state moving from the MRCI to C-MRCI+DK+Q, there is an energy difference of 1088 cm^{-1}, the final $T_e(^3\Delta \leftarrow {}^3\Phi)$ being 2329 cm^{-1}, so the $^3\Delta$ is just 110 cm^{-1} above the $^3\Pi$ state. Clearly the $^3\Pi$ and $^3\Delta$ states are degenerate within the accuracy of our calculations. The same results are obtained using the much larger C5Z/A5Z basis set, Table V.

As a final conclusion for the TiF^+ cation it can be stated that two states, $^3\Sigma^-$ and $^3\Phi$, compete strongly for being the ground state with an energy separation perhaps no more than 1 kcal/mol, and two degenerate states of symmetry $^3\Pi$ and $^3\Delta$ are located $\approx 2200-2300$ cm^{-1} higher.

3. VF^+

No experimental or any kind of theoretical results on VF^+ exist in the literature. We have examined five states, two $^4\Pi$s one of which is the ground state, plus three more low-lying states of $^4\Delta$, $^4\Sigma^-$, and $^4\Phi$ symmetry, as shown in

TABLE V. Results on the $X\,^3\Phi$, $A\,^3\Sigma^-$, $B\,^3\Pi$, and $C\,^3\Delta$ states of TiF^+ using the series of correlation consistent-type basis sets on Ti and the corresponding aug-cc-basis on F. Symbols, units, and acronyms as in Table I.

Basis set[a]	Method	$-E$	r_e	D_e	ω_e	$\omega_e x_e$	T_e
		$X\,^3\Phi$					
QZ/AQZ	MRCI	948.058 76	1.799	125.2	742	3.1	0.0
	MRCI+Q	948.076 53	1.799	129.7	743	3.1	0.0
CQZ/AQZ	C-MRCI	948.367 07	1.779	122.2			0.0
	C-MRCI+Q	948.425 74	1.775	128.7			0.0
5Z/A5Z	MRCI	948.068 14	1.798	125.7	744	3.0	0.0
	MRCI+Q	948.086 21	1.798	130.3	744	3.1	0.0
	RCCSD(T)	948.087 00	1.812	129.3			0.0
C5Z/A5Z	C-MRCI	948.386 19	1.777	123.0			0.0
	C-MRCI+Q	948.446 18	1.773	129.6			0.0
	C-MRCI+DK	952.813 94	1.778	120.4			0.0
	C-MRCI+DK+Q	952.874 00	1.774	126.6			0.0
	C-RCCSD(T)	948.454 86	1.775	132.4			0.0
		$A\,^3\Sigma^-$					
QZ/AQZ	MRCI	948.056 03	1.770	124.2	740	3.3	598
	MRCI+Q	948.074 18	1.767	129.0	741	3.1	514
CQZ/AQZ	C-MRCI	948.366 20	1.749	121.8			192
	C-MRCI+Q	948.426 06	1.742	129.0			−70
5Z/A5Z	MRCI	948.065 45	1.769	124.7	741	2.9	591
	MRCI+Q	948.083 90	1.766	129.5	742	2.9	507
	RCCSD(T)	948.087 37	1.777	129.5			−80
C5Z/A5Z	C-MRCI	948.385 28	1.747	122.6			199
	C-MRCI+Q	948.446 46	1.740	129.9			−59
	C-MRCI+DK	952.812 73	1.748	119.8			266
	C-MRCI+DK+Q	952.874 39	1.741	126.8			−87
	C-RCCSD(T)	948.458 80	1.728	134.9			−864
		$B\,^3\Pi$					
QZ/AQZ	MRCI	948.047 55	1.807	118.4	727	3.0	2459
	MRCI+Q	948.065 79	1.806	123.2	728	3.0	2357
CQZ/AQZ	C-MRCI	948.355 98	1.786	115.3			2434
	C-MRCI+Q	948.415 33	1.781	122.2			2283
5Z/A5Z	MRCI	948.056 93	1.807	118.9	728	3.0	2459
	MRCI+Q	948.075 47	1.805	123.7	728	2.8	2357
C5Z/A5Z	C-MRCI	948.375 01	1.785	116.1			2452
	C-MRCI+Q	948.435 66	1.779	123.1			2308
		$C\,^3\Delta$					
QZ/AQZ	MRCI	948.043 21	1.796	115.2	665	0.7	3414
	MRCI+Q	948.063 00	1.787	121.0	663	1.1	2969
CQZ/AQZ	C-MRCI	948.350 28	1.774	111.6			3683
	C-MRCI+Q	948.411 71	1.757	119.9			3081
5Z/A5Z	MRCI	948.052 55	1.796	115.6	666	0.9	3421
	MRCI+Q	948.072 62	1.786	121.4	665	1.4	2983
C5Z/A5Z	C-MRCI	948.369 08	1.773	112.2			3753
	C-MRCI+Q	948.431 77	1.757	120.5			3162

[a]See text.

Fig. 4 and Table VI. The $X\,^4\Pi$ and $^4\Delta$ states correlate adiabatically to the ground state atoms V^+ $(a\,^5D)+F(^2P)$, while the rest three to the first excited state of V^+, $a\,^5F$. Differences of about $0.003E_h$ observed at infinity within the same dissociation channel, Fig. 4, are rather due to the state-average technique between the $X\,^4\Pi+{}^4\Phi+{}^4\Pi(2)$ (B_1, B_2 symmetries under C_{2v}), and $A\,^4\Delta+B\,^4\Sigma^-$ (A_1,A_2). This $0.003E_h$ diminishes to about $0.001E_h$ at the $+Q$ level. The asymptotic energy difference between the two channels obtained by the supermolecule approach and reflecting the V^+ $a\,^5F$-$a\,^5D$ splitting at the MRCI($+Q$) level, is 2330 (2306) cm^{-1} as contrasted to the experimental one[9] of 2756 cm^{-1}.

The dissociation energy of the $X\,^4\Pi$ state is practically method independent according to the numbers of Table VI. At the highest multireference level, C-MRCI+DK+Q, D_e = 115.4 kcal/mol; the same value is obtained at the C-RCCSD(T) level+DK effects as obtained from the C-MRCI, i.e., 113.9+1.9=115.8 kcal/mol. Therefore, the recommended D_e value is 116 kcal/mol at r_e=1.734 Å.

The situation for the next two states $^4\Delta$ and $^4\Sigma^-$ is rather unclear as to their relative ordering, Table VI. The symmetry problem on the first excited state is also compounded by the fact that the $^4\Delta$ and $^4\Sigma^-$ states correlate to different atomic states. The MRCI ($+Q$) $\Delta E(^4\Sigma^- \leftarrow {}^4\Delta)$ is 740 (7) cm^{-1}. This ordering is maintained at the C-MRCI

TABLE VI. Results on the $X\ ^4\Pi$, $A\ ^4\Delta$, $B\ ^4\Sigma^-$, $C\ ^4\Phi$, and $D\ ^4\Pi$ states of VF^+. Symbols, units, and acronyms as in Table I.

Method	$-E$	r_e	D_e	ω_e	$\omega_e x_e$	α_e	q_V	T_e
			$X\ ^4\Pi$					
MRCI	1042.536 24	1.756	113.9	753	3.0	0.0025	1.58	0.0
MRCI+Q	1042.557 43	1.753	115.2	755	3.0	0.0025		0.0
MRACPF	1042.554 03	1.753	114.7	756	3.6	0.0025	1.57	0.0
MRCI+DK	1047.869 70	1.753	117.1	753	2.5	0.0026	1.69	0.0
MRCI+DK+Q	1047.891 02	1.750	118.5	757	3.0	0.0025		0.0
C-MRCI	1042.826 48	1.742	110.5	771	3.1	0.0025	1.61	0.0
C-MRCI+Q	1042.886 14	1.734	113.1	780	3.4	0.0025		0.0
C-MRCI+DK	1048.206 17	1.741	112.4	771	3.4	0.0026	1.70	0.0
C-MRCI+DK+Q	1048.269 47	1.734	115.4	783	7.5	0.0029		0.0
RCCSD(T)	1042.562 79	1.753	114.1	758	3.2	0.0025		0.0
C-RCCSD(T)	1042.898 90	1.732	113.9	781	3.2	0.0026		0.0
			$A\ ^4\Delta$					
MRCI	1042.529 76	1.786	107.7	743	3.3	0.0024	1.62	1423
MRCI+Q	1042.549 39	1.785	109.5	740	2.3	0.0027		1763
MRACPF	1042.546 29	1.786	108.6	736	4.9	0.0030	1.60	1696
MRCI+DK	1047.862 74	1.784	110.6	742	2.6	0.0023	1.71	1528
MRCI+DK+Q	1047.882 51	1.783	112.5	743	3.0	0.0023		1868
C-MRCI	1042.818 87	1.773	103.6	754	2.3	0.0024	1.63	1668
C-MRCI+Q	1042.876 24	1.769	106.6	761	3.1	0.0023		2172
C-MRCI+DK	1048.198 26	1.773	105.2	756	4.3	0.0026	1.72	1735
C-MRCI+DK+Q	1048.259 36	1.770	108.4	760	4.3	0.0025		2217
RCCSD(T)	1042.555 70	1.787	109.7	744	3.0	0.0024		1553
C-RCCSD(T)	1042.890 42	1.770	108.6	761	3.4	0.0023		1861
			$B\ ^4\Sigma^-$					
MRCI	1042.526 39	1.771	114.7	724	3.0	0.0022	1.60	2165
MRCI+Q	1042.549 36	1.764	119.7	725	2.8	0.0022		1770
MRACPF	1042.543 93	1.768	117.4	717	0.8	0.0025	1.55	2217
MRCI+DK	1047.861 08	1.763	113.4	723	2.6	0.0022	1.68	1892
MRCI+DK+Q	1047.884 24	1.755	118.5	724	2.3	0.0021		1490
C-MRCI	1042.815 76	1.758	111.7	737	3.0	0.0021	1.63	2354
C-MRCI+Q	1042.876 93	1.746	118.1	743	2.8	0.0021		2022
C-MRCI+DK	1048.196 79	1.752	108.2	738	5.3	0.0023	1.71	2057
C-MRCI+DK+Q	1048.261 70	1.739	114.2	743	5.5	0.0022		1703
RCCSD(T)	1042.555 83	1.767	118.8	726	2.9	0.0022		1528
C-RCCSD(T)	1042.891 43	1.740	120.1	746	2.8	0.0021		1640
			$C\ ^4\Phi$					
MRCI	1042.510 99	1.800	102.5	691	2.5	0.0020	1.62	5544
MRCI+Q	1042.532 83	1.794	107.8	692	2.6	0.0021		5400
MRCI+DK	1047.845 88	1.790	101.4	691	2.5	0.0019	1.69	5229
MRCI+DK+Q	1047.868 00	1.783	106.8	691	2.5	0.0020		5054
C-MRCI	1042.799 82	1.785	99.7	705	2.9	0.0020	1.63	5851
C-MRCI+Q	1042.859 68	1.774	106.7	707	2.5	0.0020		5809
C-MRCI+DK	1048.181 09	1.778	96.4	702	3.8	0.0021	1.71	5502
C-MRCI+DK+Q	1048.244 87	1.765	103.2	703	2.4	0.0020		5397
			$D\ ^4\Pi$					
MRCI	1042.476 61	1.772	81.0	727	2.9	0.0020	1.59	13 088
MRCI+Q	1042.501 15	1.766	88.0	727	2.6	0.0020		12 350
MRCI+DK	1047.811 76	1.762	80.1	725	2.7	0.0019	1.67	12 717
MRCI+DK+Q	1047.836 54	1.755	87.1	724	2.0	0.0020		11 958
C-MRCI	1042.768 77	1.762	80.2	734	2.7	0.0019	1.61	12 665
C-MRCI+Q	1042.832 58	1.752	89.8	737	2.4	0.0019		11 755
C-MRCI+DK	1048.149 95	1.754	76.9	729	2.1	0.0017	1.70	12 339
C-MRCI+DK+Q	1048.217 52	1.743	86.1	730	0.9	0.0017		11 398

level ($\Delta E = 683\ cm^{-1}$), but it is reversed at the C-MRCI+Q, C-MRCI+DK+Q, RCCSD(T) and C-RCCSD(T) levels of theory by 151, 513, 29, and 222 cm^{-1}, respectively. Obviously, the safe conclusion at this point is that these two states are degenerate, or that their ''real'' energy difference should be close to 1 kcal/mol. Of course the ordering given in Table VI is only formal. Recommended binding energies are 110 ($^4\Delta$) and 116 ($^4\Sigma^-$) kcal/mol with respect to the adiabatic fragments.

The ordering of the next two states is clear, $C\ ^4\Phi$ fol-

lowed by $D\,^4\Pi$. The $C\,^4\Phi$-$X\,^4\Pi$ and $D\,^4\Pi$-$X\,^4\Pi$ T_e values are method independent within the accuracy of our methods. Suggested T_e and D_e values for the $C\,^4\Phi$ and $D\,^4\Pi$ states of VF^+ are 16, 35 kcal/mol and 105, 86 kcal/mol, respectively.

4. CrF^+

We report ten states of the CrF^+ cation, three of which $X\,^5\Sigma^+$, $A\,^5\Pi$, and $B\,^5\Delta$ are well separated and approximately equally spaced, while the remaining seven are crowded within an energy range of about 4000 cm^{-1}; see Fig. 5. The only experimental result available is the ionization energy, IE $=8.4\pm0.3$ eV of CrF,[8] which allows the estimation of the dissociation energy of CrF^+, $D_0=68.6\pm10.4$ kcal/mol (see Sec. I). Our results indicate a significantly larger D_e value, the error being traced to the high experimentally determined IE.[8] Indeed, from the results of Ref. 1 we obtain IE(CrF) $=7.81$ (7.77) [7.89] eV at the C-MRCI+Q (C-MRCI+DK+Q) [C-RCCSD(T)] level, all values significantly lower than the experimental one. Therefore, using an IE (CrF) $=7.9$ eV, D_e (CrF; $X\,^6\Sigma^+$) $=110$ kcal/mol,[1] and IE (Cr) $=6.77$ eV,[9] we expect a dissociation energy of CrF^+ close to 85 kcal/mol.

The $X\,^5\Sigma^+$ state of CrF^+ is the only one which correlates adiabatically to the ground state fragments, Cr^+ (^6S) $+F(^2P)$; Table IX and Fig. 5. Following the results of Table VII a monotonic decrease of bond distance is observed, albeit small, from 1.734 Å (MRCI) to 1.722 Å (C-MRCI $+DK+Q$). Exactly the same number is obtained at the C-RCCSD(T)+DK level. However, D_e values show a diference of up to 10% depending on the method. It is interesting though that the DK effects are practically the same in both MRCI, RCCSD(T) and C-MRCI, C-RCCSD(T) methods. Taking everything into account our best D_e estimate is 87 kcal/mol, or $D_0=86$ kcal/mol and $r_e=1.722$ Å.

The first excited state, $A\,^5\Pi$, correlates adiabatically to the first excited state of the Cr^+ (^6D) cation, experimentally located 12 278 cm^{-1} above the ^6S term.[9] Our MRCI ^6D-^6S splitting using the supermolecule approach is 12 000 cm^{-1}. Concerning the bond distance we observe the same monotonical reduction as before moving from the MRCI ($r_e=1.762$ Å) to C-MRCI+DK+Q ($r_e=1.737$ Å) to C-RCCSD(T)+DK ($r_e=1.736$ Å). What is rather difficult to obtain again is the estimation of the dissociation energy. The results of relativity in this state have an opposite effect reducing the binding energy as compared to the $X\,^5\Sigma^+$ state. Disregarding the C-MRCI values because of high nonextensivity errors, the MRCI+DK+Q and C-RCCSD(T)+DK numbers are in good agreement. Therefore, our estimate for the D_e (D_0) value is 107 (106) kcal/mol, with T_e ($A\,^5\Pi \leftarrow X\,^5\Sigma^+$) $\sim$4100 cm^{-1}, the mean value of these two methods.

The $B\,^5\Delta$ is located $\approx$10 000 cm^{-1} above the X state tracing its origin to Cr^+ (^6D) $+F(^2P)$. As in the previous two states the C-MRCI+DK and C-RCCSD(T)+DK r_e values are in excellent agreement, 1.778 versus 1.775 Å, respectively. Also in agreement are the D_e MRCI+DK+Q and C-RCCSD(T)+DK values, so our best estimate of the dissociation energy is $D_e(D_0)=92$ (91) kcal/mol, and T_e $(B\,^5\Delta \leftarrow X\,^5\Sigma^+)=(9\,485+9\,729)/2\sim9\,600$ cm^{-1}.

The band of the remaining seven triplets tagged only formally at the MRCI level as $a\,^3\Gamma$, $b\,^3\Phi$, $c\,^3\Sigma^-$, $d\,^3\Pi$, $e\,^3\Delta$, $f\,^3H$, and $g\,^3\Sigma^+$, correlates adiabatically to Cr^+ $(^4D)+F(^2P)$ [$d\,^3\Pi$, $e\,^3\Delta$, $g\,^3\Sigma^+$], to Cr^+ $(^4G)+F(^2P)$ [$a\,^3\Gamma$,$b\,^3\Phi$], and to Cr^+ $(^4P)+F(^2P)$ [$c\,^3\Sigma^-$], but we are not sure as to the end products of the $f\,^3H$ state. For technical reasons we were not able to complete the PECs of the $^3\Gamma$, $^3\Phi$, $^3\Sigma^-$, and ^3H states beyond an internuclear distance of 5 bohrs; see Fig. 5. In higher resolution the band of these seven states above is composed of three groups of two ($a\,^3\Gamma$,$b\,^3\Phi$), two ($c\,^3\Sigma^-$,$d\,^3\Pi$), and three ($e\,^3\Delta$,$f\,^3H$, $g\,^3\Sigma^+$) states, practicaly degenerate within each group; Fig. 5 and Table VII. We are rather sure of the ordering of the three groups but obviously not within the groups. Note that for the states $^3\Gamma$, $^3\Phi$, $^3\Sigma^-$, and ^3H, D_e entries are missing from Table VII due to our inability to calculate the supermolecular states at the correct adiabatic limits.

A general observation is useful at this point. It was mentioned in the introduction that the bonding and states of the MF^+ species can be understood with an *in situ* ionic description $M^{2+}F^-$. This is particularly clear in the CrF^+ and MnF^+ cases. The ground term of Cr^{2+} is ^5D ($3d^4$) which can give rise to three low-lying states of $^5\Sigma^+$, $^5\Pi$, and $^5\Delta$ symmetry in the field of F^-. This is exactly what we see in Fig. 5. Now, two, in essence degenerate states of Cr^{2+}, ^3F, and ^3H, lie 17 100 cm^{-1} above its ^5D state.[9] The ^3H term, formally the lower, can give rise to a series of closely spaced molecular states of $^3\Sigma^-$, $^3\Pi$, $^3\Delta$, $^3\Phi$, $^3\Gamma$, and ^3H symmetry. The $^3\Sigma^+$ can be considered as arising from the $^3G(3d^4)$ of Cr^{2+}, 20 521 cm^{-1} above the ^5D term. Indeed, the band average of the presently calculated seven states of the same symmetry is located $\sim$16 000 cm^{-1} above the average of the lowest $X\,^5\Sigma^+$, $A\,^5\Pi$, and $B\,^5\Delta$ states at the MRCI level of theory. The agreement within $\sim$1000 cm^{-1} of the Cr^{2+} atomic terms and corresponding molecular CrF^+ states is striking, leaving little doubt as to the $M^{2+}F^-$ description of these systems.

5. MnF^+

We are not aware of any published theoretical results on MnF^+. Experimentally, the ionization energy of the neutral MnF has been reported by Margrave and co-workers,[38] IE $=8.7\pm0.3$ eV; in the same work the dissociation energy of MnF is also given, $D_0=101.2\pm3.5$ kcal/mol. Using the experimental ionization energy of Mn, IE $=7.43$ eV,[9] the experimental D_0 value of MnF^+ can be obtained via formula (1) of the Introduction.

$$D_0\ (MnF^+)=101.2\ \text{kcal/mol}+7.43\ \text{eV}-8.7\pm0.3\ \text{eV}$$

$$=71.9\pm10.4\ \text{kcal/mol}.$$

Upgrading the above estimate by the most recent dissociation energy of MnF,[33] $D_0=106.4\pm1.8$ kcal/mol, also in agreement with the results of Ref. 1, we obtain, D_0 (MnF^+) $=77.1\pm8.7$ kcal/mol. Disregarding the error bars, this experimental D_0 value of MnF^+ is low by at least 10 kcal/mol

TABLE VII. Results on the $X\ ^5\Sigma^+$, $A\ ^5\Pi$, $B\ ^5\Delta$, $a\ ^3\Gamma$, $b\ ^3\Phi$, $c\ ^3\Sigma^-$, $d\ ^3\Pi$, $e\ ^3\Delta$, $f\ ^3H$, and $g\ ^3\Sigma^+$ states of CrF^+. Symbols, units, and acronyms as in Table I.

Method	$-E$	r_e	D_e	ω_e	$\omega_e x_e$	α_e	q_{Cr}	T_e
			$X\ ^5\Sigma^+$					
MRCI	1142.982 14	1.734	82.5	781	3.1	0.0025	1.59	0.0
MRCI+Q	1143.005 35	1.732	83.1	781	2.6	0.0024		0.0
MRACPF	1143.001 87	1.733	81.7	775	2.2	0.0024	1.56	0.0
MRCI+DK	1149.368 22	1.732	86.0	785	3.3	0.0025	1.68	0.0
MRCI+DK+Q	1149.391 57	1.730	86.8	784	3.1	0.0024		0.0
C-MRCI	1143.287 79	1.726	80.9	795	3.1	0.0024	1.62	0.0
C-MRCI+Q	1143.349 10	1.721	82.9	800	3.3	0.0025		0.0
C-MRACPF	1143.344 53	1.723	79.1				1.59	0.0
C-MRCI+DK	1149.719 90	1.726	83.1	794	3.3	0.0025	1.70	0.0
C-MRCI+DK+Q	1149.784 61	1.722	85.2	797	3.3	0.0025		0.0
RCCSD(T)	1143.013 37	1.732	83.9	785	3.3	0.0025		0.0
RCCSD(T)+DK	1149.399 83	1.730	87.6	787	3.3	0.0026		0.0
C-RCCSD(T)	1143.366 42	1.721	85.1	801	3.4	0.0025		0.0
C-RCCSD(T)+DK	1149.804 42	1.722	86.7					0.0
			$A\ ^5\Pi$					
MRCI	1142.959 44	1.762	101.3	739	2.9	0.0022	1.61	4982
MRCI+Q	1142.984 90	1.756	108.0	742	3.0	0.0023		4488
MRACPF	1142.979 86	1.759	105.9	739	3.4	0.0023	1.57	4831
MRCI+DK	1149.347 11	1.755	99.5	742	3.3	0.0023	1.68	4634
MRCI+DK+Q	1149.372 79	1.748	106.2	743	2.8	0.0023		4122
C-MRCI	1143.263 67	1.752	98.2	752	3.2	0.0023	1.63	5293
C-MRCI+Q	1143.326 72	1.743	106.4	760	3.4	0.0023		4912
C-MRACPF	1143.321 08	1.747	105.2				1.57	5148
C-MRCI+DK	1149.697 45	1.747	94.1	749	3.1	0.0023	1.71	4928
C-MRCI+DK+Q	1149.764 01	1.737	102.1	755	3.0	0.0023		4522
RCCSD(T)	1142.992 68	1.757	110.3	739	2.7	0.0024		4540
RCCSD(T)+DK	1149.380 89	1.748	108.6	744	3.1	0.0023		4157
C-RCCSD(T)	1143.345 93	1.741	111.4	755	2.9	0.0024		4497
C-RCCSD(T)+DK	1149.785 98	1.736	107.6					4046
			$B\ ^5\Delta$					
MRCI	1142.936 87	1.802	88.4	701	2.9	0.0022	1.64	9935
MRCI+Q	1142.960 20	1.797	93.1	701	2.9	0.0022		9910
MRACPF	1142.957 33	1.800	92.4	699	3.2	0.0022	1.60	9775
MRCI+DK	1149.324 70	1.794	86.7	702	2.8	0.0022	1.70	9551
MRCI+DK+Q	1149.348 36	1.789	91.5	703	3.1	0.0022		9485
C-MRCI	1143.241 42	1.791	85.7	711	2.8	0.0022	1.66	10 177
C-MRCI+Q	1143.302 41	1.784	92.0	716	3.3	0.0022		10 246
C-MRACPF	1143.299 10	1.787	92.3				1.59	9971
C-MRCI+DK	1149.675 48	1.786	81.7	709	2.9	0.0022	1.73	9750
C-MRCI+DK+Q	1149.740 20	1.778	87.8	713	3.2	0.0022		9748
RCCSD(T)	1142.967 46	1.797	94.5	702	3.5	0.0024		10 076
RCCSD(T)+DK	1149.355 91	1.789	93.0	703	2.9	0.0023		9640
C-RCCSD(T)	1143.319 67	1.780	95.0	716	3.0	0.0022		10 261
C-RCCSD(T)+DK	1149.760 09	1.775	91.3					9729
			$a\ ^3\Gamma$					
MRCI	1142.896 08	1.725		791	2.9	0.0025	1.59	18 888
MRCI+Q	1142.920 94	1.723		793	3.1	0.0024		18 526
MRACPF	1142.917 83	1.726		787	3.0	0.0024	1.54	18 445
MRCI+DK	1149.283 48	1.723		793	3.2	0.0025	1.68	18 598
MRCI+DK+Q	1149.308 49	1.721		796	3.5	0.0025		18 234
C-MRCI	1143.204 39	1.716		806	3.3	0.0025	1.61	18 304
C-MRCI+Q	1143.267 82	1.711		812	3.0	0.0024		17 839
C-MRCI+DK	1149.637 80	1.716		802	3.0	0.0026	1.70	18 018
C-MRCI+DK+Q	1149.704 72	1.712		803	1.5	0.0025		17 534
			$b\ ^3\Phi$					
MRCI	1142.895 12	1.717		775	3.0	0.0025	1.58	19 099
MRCI+Q	1142.920 75	1.712		780	3.1	0.0025		18 568
MRACPF	1142.916 52	1.715		773	3.0	0.0025	1.55	18 732
MRCI+DK	1149.282 84	1.714		777	3.0	0.0025	1.67	18 738
MRCI+DK+Q	1149.308 67	1.708		781	3.0	0.0025		18 194
C-MRCI	1143.203 01	1.709		788	3.1	0.0025	1.60	18 607
C-MRCI+Q	1143.267 49	1.701		798	3.2	0.0025		17 911

TABLE VII. (*Continued*.)

Method	$-E$	r_e	D_e	ω_e	$\omega_e x_e$	α_e	q_{Cr}	T_e
C-MRCI+DK	1149.636 63	1.709		782	2.0	0.0025	1.69	18 348
C-MRCI+DK+Q	1149.704 62	1.700		795	3.1	0.0025		17 556
			$c\ ^3\Sigma^-$					
MRCI	1142.887 87	1.725		792	3.1	0.0025	1.59	20 690
MRCI+Q	1142.916 09	1.725		791	3.1	0.0025		19 590
MRACPF	1142.913 66	1.730					1.55	19 360
C-MRCI	1143.192 78	1.716					1.60	20 852
C-MRCI+Q	1143.260 43	1.713						19 461
			$d\ ^3\Pi$					
MRCI	1142.885 63	1.708	77.2	738	4.7	0.0054	1.56	21 181
MRCI+Q	1142.912 90	1.700	84.2	755	6.4	0.0052		20 290
MRACPF	1142.908 11	1.708	81.9				1.52	20 578
C-MRCI	1143.193 76	1.702	78.5				1.59	20 637
C-MRCI+Q	1143.261 03	1.693	88.0					19 329
			$e\ ^3\Delta$					
MRCI	1142.879 86	1.716	73.5	799	3.1	0.0025	1.57	22 448
MRCI+Q	1142.909 16	1.718	81.5	799	3.1	0.0025		21 111
MRACPF	1142.906 72	1.727	81.0				1.52	20 883
C-MRCI	1143.187 81	1.712	74.5				1.60	21 943
C-MRCI+Q	1143.255 96	1.708	84.7					20 442
			$f\ ^3\mathrm{H}$					
MRCI	1142.877 69	1.752		748	3.9	0.0024	1.60	22 924
MRCI+Q	1142.904 58	1.744		751	3.2	0.0023		22 116
MRACPF	1142.899 50	1.751					1.55	22 468
C-MRCI	1143.185 72	1.744					1.62	22 402
C-MRCI+Q	1143.251 30	1.733						21 465
			$g\ ^3\Sigma^+$					
MRCI	1142.876 11	1.719	71.2	800	3.5	0.0025	1.57	23 271
MRCI+Q	1142.903 04	1.717	77.8	799	3.1	0.0026		22 454
MRACPF	1142.899 40	1.722	76.5				1.52	22 490
C-MRCI	1143.186 15	1.713	73.6				1.60	22 307
C-MRCI+Q	1143.252 68	1.709	82.6					21 162

according to present results (*vide infra*), the error being traced to the high ionization energy of MnF by about 0.5 eV (see also the CrF^+ section).

We have calculated seven states of MnF^+, the ground $X\ ^6\Sigma^+$, and a closely spaced band of six states, Fig. 6. Following the analysis of the previous section on TiF^+ and CrF^+, the Mn^{2+} cation is characterized by a $^6S(3d^5)$ ground state followed by two terms of ^4G and ^4P symmetry, 26 845 and 29 193 cm^{-1} higher, respectively.[9] Therefore, in the field of F^-, we expect the formation of an "isolated" $^6\Sigma^+$ state followed by a rather closely spaced band of states of $^4\Sigma^+$, $^4\Pi$, $^4\Delta$, $^4\Phi$, and $^4\Gamma$ symmetry. This is exactly what we see in Fig. 6. Remarkably, the band center of these five states is located 26 460 cm^{-1} above the $X\ ^6\Sigma^+$ state at the MRCI level, in complete agreement with the Mn^{2+} (^4G-^6S) splitting. The extra $e\ ^5\Pi$ state, 28 500 cm^{-1} (MRCI) higher, is related to the ^4P term of Mn^{2+}.

Again, the standard spectroscopic naming of the quartet states is based on the MRCI findings and it is only formal.

From Table VIII it is seen that the bond length of the $X\ ^6\Sigma^+$ state converges relatively smoothly to a C-MRCI+DK+Q value of 1.750 Å. The situation is not so clear for the dissociation energy which shows considerable variations due to size nonextensivity errors at the multireference approach. Nevertheless, at the highest level C-MRCI+DK+Q and taking also into account the MRCI+DK+Q results, we can claim that the D_e is higher than 85 kcal/mol. Correcting the RCCSD(T) [C-RCCSD(T)] D_e value for relativistic effects using the MRCI+DK−MRCI [C-MRCI+DK−C-MRCI] results, −2.3 kcal/mol [−4.9 kcal/mol], we obtain D_e=91.7 kcal/mol [90.9 kcal/mol]. Our obvious recommendation at this point is that the dissociation energy of MnF^+ ($X\ ^6\Sigma^+$) with respect to the ground state fragments should be very close to 92 kcal/mol or a little bit higher. This number can be corroborated by applying formula (1) using the following results: D_0 (MnF)=106.4±1.8 kcal/mol (Ref. 33) (theoretical value D_e=108 kcal/mol[1]) and IE (Mn) =7.43 eV.[9] Our uncertainty comes from the calculated ionization energy of MnF ($X\ ^7\Sigma^+$): At the C-MRCI+Q (C-MRCI+DK+Q) [C-RCCSD(T)] level, IE (MnF)=7.95 (8.05) [7.90] eV (Ref. 1 and present work), so it is rather safe to use IE=8.0±0.1 eV. Therefore, D_0=106.4±1.8 kcal/mol+7.43 eV−8.0±0.1 eV=93.3±4.1 kcal/mol, consistent with the suggested theoretical value of 92 kcal/mol.

Not much can be said about the band of six quartet states; it is composed of three groups of two states each, ($a\ ^4\Delta$,$b\ ^4\Pi$), ($c\ ^4\Phi$,$d\ ^4\Sigma^+$), and ($e\ ^4\Pi$,$f\ ^4\Gamma$), practically

TABLE VIII. Results on the $X\,^6\Sigma^+$, $a\,^4\Delta$, $b\,^4\Pi(1)$, $c\,^4\Phi$, $d\,^4\Sigma^+$, $e\,^4\Pi(2)$, and $f\,^4\Gamma$ states of MnF^+. Symbols, units, and acronyms as in Table I.

Method	$-E$	r_e	D_e[a]	ω_e	$\omega_e x_e$	α_e	q_{Mn}	T_e
			$X\,^6\Sigma^+$					
MRCI	1249.516 24	1.769	86.3	730	3.1	0.0023	1.64	0.0
MRCI+Q	1249.541 70	1.765	91.5	728	2.6	0.0024		0.0
MRACPF	1249.538 90	1.768	90.8	725	2.7	0.0023	1.60	0.0
MRCI+DK	1257.110 29	1.762	84.0	731	2.9	0.0024	1.74	0.0
MRCI+DK+Q	1257.136 11	1.758	89.3	731	2.8	0.0024		0.0
C-MRCI	1249.825 40	1.760	83.9	742	3.1	0.0024	1.66	0.0
C-MRCI+Q	1249.886 83	1.754	90.5	743	2.3	0.0024		0.0
C-MRCI+DK	1257.470 34	1.756	79.0	736	3.0	0.0023	1.77	0.0
C-MRCI+DK+Q	1257.535 78	1.750	85.6	742	3.3	0.0023		0.0
RCCSD(T)	1249.549 19	1.764	94.0					0.0
C-RCCSD(T)	1249.907 87	1.750	95.8					0.0
			$a\,^4\Delta$					
MRCI	1249.404 72	1.696	67.0	781	3.5	0.0028	1.58	24 475
MRCI+Q	1249.434 71	1.691	69.3	790	4.5	0.0027		23 480
MRACPF	1249.430 83	1.692	66.9	783	3.9	0.0029	1.54	23 717
C-MRCI	1249.719 35	1.690	67.2	790	2.9	0.0029	1.61	23 276
C-MRCI+Q	1249.787 54	1.682	70.5	804	3.5	0.0029		21 793
MRCI+DK	1256.999 70	1.693		784	3.6	0.0028	1.71	24 269
MRCI+DK+Q	1257.029 94	1.688		792	4.2	0.0026		23 301
C-MRCI+DK	1257.364 69	1.691		795	9.5	0.0026	1.74	23 186
C-MRCI+DK+Q	1257.436 66	1.683		800	2.7	0.0029		21 755
			$b\,^4\Pi$					
MRCI	1249.401 00	1.726	69.0	777	3.7	0.0026	1.60	25 292
MRCI+Q	1249.429 95	1.722	67.4	780	3.5	0.0026		24 525
MRACPF	1249.427 14	1.723	65.1	774	2.8	0.0025	1.57	24 527
MRCI+DK	1256.995 48	1.723		781	4.7	0.0026	1.72	25 196
MRCI+DK+Q	1257.024 68	1.719		781	3.5	0.0025		24 456
C-MRCI	1249.715 77	1.719	69.5	788	3.7	0.0025	1.62	24 061
C-MRCI+Q	1249.783 15	1.712	68.7	797	3.7	0.0026		22 754
C-MRCI+DK	1257.360 67	1.720					1.74	24 071
C-MRCI+DK+Q	1257.431 87	1.713						22 806
			$c\,^4\Phi$					
MRCI	1249.393 50	1.731	99.6	754	2.9	0.0023	1.61	26 937
MRCI+Q	1249.423 83	1.723	106.0	761	3.1	0.0025		25 869
MRACPF	1249.419 11	1.728	104.1	757	4.0	0.0025	1.56	26 289
MRCI+DK	1256.989 20	1.725	95.5	756	2.6	0.0024	1.72	26 575
MRCI+DK+Q	1257.019 83	1.717	102.6	763	3.2	0.0025		25 521
C-MRCI	1249.708 28	1.725	97.5	766	3.7	0.0025	1.63	25 706
C-MRCI+Q	1249.776 24	1.714	105.0	777	4.2	0.0026		24 273
C-MRCI+DK	1257.354 46	1.722	90.4				1.75	25 432
C-MRCI+DK+Q	1257.426 31	1.711	98.4					24 026
			$d\,^4\Sigma^+$					
MRCI	1249.392 41	1.737	35.5	737	1.6	0.0022	1.60	27 177
MRCI+Q	1249.423 20	1.727	43.0	745	3.1	0.0023		26 007
MRACPF	1249.419 80	1.727	41.8	741	3.5	0.0023	1.54	26 138
MRCI+DK	1256.988 35	1.729	35.6	741	3.1	0.0023	1.72	26 762
MRCI+DK+Q	1257.019 53	1.718	43.1	750	4.4	0.0023		25 585
C-MRCI	1249.706 28	1.733	38.1	750	3.2	0.0023	1.62	26 144
C-MRCI+Q	1249.774 54	1.721	47.7	756	2.6	0.0023		24 645
C-MRCI+DK	1257.352 67	1.729	35.5	745			1.75	25 826
C-MRCI+DK+Q	1257.424 85	1.717	44.8	747				24 346
			$e\,^4\Pi$					
MRCI	1249.386 70	1.726	95.3	764	2.7	0.0024	1.60	28 431
MRCI+Q	1249.419 45	1.719	103.2	772	2.8	0.0024		26 831
MRACPF	1249.413 76	1.722	100.7	767	3.6	0.0025	1.54	27 465
MRCI+DK	1256.983 04	1.719	91.5	768	3.3	0.0026	1.72	27 927
MRCI+DK+Q	1257.016 11	1.711	100.1	776	3.2	0.0025		26 335
C-MRCI	1249.700 53	1.716	92.6	775	2.6	0.0025	1.63	27 407
C-MRCI+Q	1249.771 34	1.709	101.9	790	4.1	0.0025		25 347
C-MRCI+DK	1257.347 13	1.715	85.8				1.75	27 041
C-MRCI+DK+Q	1257.421 81	1.705	95.5					25 014
			$f\,^4\Gamma$					
MRCI	1249.386 31	1.754	93.4	739	3.1	0.0025	1.63	28 515
MRCI+Q	1249.414 58	1.748	99.0	744	3.6	0.0023		27 898
MRACPF	1249.411 30	1.751	97.9	738	3.0	0.0023	1.58	28 005
MRCI+DK	1256.981 89	1.747	91.2	740	3.0	0.0024	1.73	28 179
MRCI+DK+Q	1257.010 55	1.741	96.8	741	2.0	0.0023		27 556
C-MRCI	1249.702 10	1.745	91.9	754	3.2	0.0024	1.64	27 062
C-MRCI+Q	1249.768 34	1.737	99.0	759	3.1	0.0024		26 005
C-MRCI+DK	1257.348 32	1.742	87.1	754			1.76	26 780
C-MRCI+DK+Q	1257.418 64	1.734	94.0	762				25 710

TABLE IX. Asymptotic fragments M^+, leading CASSCF configurations CF, and CASSCF Mulliken atomic populations of all MF^+ states studied, M = Sc, Ti, V, Cr, and Mn.

State	Asymptotic fragment, M^+	Leading CASSCF CFs	M							F			
			$4s$	$4p_z$	$3d_{z^2}$	$3d_{xz}$	$3d_{yz}$	$3d_{x^2-y^2}$	$3d_{xy}$	$2s$	$2p_z$	$2p_x$	$2p_y$
		ScF^+											
$X\,^2\Delta$	$\|^3D;\ M_L=\pm2\rangle$	$0.997\|1\delta_+^1\rangle$	0.03	0.0	0.15	0.06	0.06	0.97	0.0	1.97	1.80	1.92	1.92
$A\,^2\Sigma^+$	$\|^3D;\ M_L=0\rangle$	$0.997\|3\sigma^1\rangle$	0.56	0.02	0.64	0.06	0.06	0.0	0.0	1.96	1.82	1.91	1.91
$B\,^2\Pi$	$\|^3D;\ M_L=\pm1\rangle$	$0.997\|2\pi_x^1\rangle$	0.03	0.01	0.14	1.00	0.05	0.0	0.0	1.98	1.82	1.94	1.93
		TiF^+											
$X\,^3\Sigma^-$	$\|^4F;\ M_L=0\rangle$	$0.84\|1\delta_+^1 1\delta_-^1\rangle+0.53\|2\pi_x^1 2\pi_y^1\rangle$	0.04	0.0	0.16	0.30	0.30	0.74	0.74	1.99	1.80	1.93	1.93
$A\,^3\Phi$	$\|^4F;\ M_L=\pm3\rangle$	$1/\sqrt{2}\|2\pi_x^1 1\delta_+^1+2\pi_y^1 1\delta_-^1\rangle$	0.05	0.0	0.16	0.53	0.53	0.50	0.50	1.99	1.80	1.94	1.94
$B\,^3\Pi$	$\|^4F;\ M_L=\pm1\rangle$	$0.65\|2\pi_x^1 1\delta_+^1-2\pi_y^1 1\delta_-^1\rangle-0.37\|3\sigma^1 2\pi_x^1\rangle$	0.05	0.0	0.27	0.59	0.46	0.43	0.43	1.99	1.81	1.94	1.94
$C\,^3\Delta$	$\|^4F;\ M_L=\pm2\rangle$	$0.997\|3\sigma^1 1\delta_+^1\rangle$	0.16	0.0	0.97	0.05	0.05	1.0	0.0	1.99	1.80	1.93	1.93
		VF^+											
$X\,^4\Pi$	$\|^5D;\ M_L=\pm1\rangle$	$0.87\|2\pi_y^1 1\delta_+^1 1\delta_-^1\rangle+0.34\|3\sigma^1(2\pi_y^1 1\delta_-^1-2\pi_x^1 1\delta_+^1)\rangle$	0.07	0.0	0.36	0.17	0.91	0.88	0.88	1.98	1.80	1.92	1.92
$A\,^4\Delta$	$\|^5D;\ M_L=\pm2\rangle$	$0.996\|2\pi_x^1 2\pi_y^1 1\delta_+^1\rangle$	0.04	0.0	0.16	1.02	1.02	1.0	0.0	1.98	1.79	1.94	1.94
$B\,^4\Sigma^-$	$\|^5F;\ M_L=0\rangle$	$0.96\|3\sigma^1 1\delta_+^1 1\delta_-^1\rangle+0.27\|3\sigma^1 2\pi_x^1 2\pi_y^1\rangle$	0.11	0.0	1.02	0.12	0.12	0.93	0.93	1.97	1.84	1.92	1.92
$C\,^4\Phi$	$\|^5F;\ M_L=\pm3\rangle$	$1/\sqrt{2}\|3\sigma^1(2\pi_x^1 1\delta_+^1+2\pi_y^1 1\delta_-^1)\rangle$	0.14	0.0	1.00	0.54	0.54	0.50	0.50	1.98	1.83	1.93	1.93
$D\,^4\Pi$	$\|^5D;\ M_L=\pm1\rangle$	$0.61\|3\sigma^1(2\pi_x^1 1\delta_+^1-2\pi_y^1 1\delta_-^1)\rangle+0.49\|2\pi_y^1 1\delta_+^1 1\delta_-^1\rangle$	0.12	0.0	0.80	0.42	0.66	0.62	0.62	1.98	1.82	1.92	1.92
		CrF^+											
$X\,^5\Sigma^+$	$\|^6S;\ M_L=0\rangle$	$0.995\|2\pi_x^1 2\pi_y^1 1\delta_+^1 1\delta_-^1\rangle$	0.05	0.02	0.20	1.03	1.03	1.0	1.0	1.98	1.73	1.91	1.91
$A\,^5\Pi$	$\|^6D;\ M_L=\pm1\rangle$	$0.997\|3\sigma^1 2\pi_y^1 1\delta_+^1 1\delta_-^1\rangle$	0.12	0.04	1.02	0.10	1.03	1.0	1.0	1.98	1.80	1.85	1.91
$B\,^5\Delta$	$\|^6D;\ M_L=\pm2\rangle$	$0.997\|3\sigma^1 2\pi_x^1 2\pi_y^1 1\delta_+^1\rangle$	0.16	0.04	1.01	1.03	1.03	1.0	0.0	1.98	1.78	1.91	1.91
$a\,^3\Gamma$	$\|^4G;\ M_L=\pm4\rangle$	$0.81\|2\pi_x^1 2\pi_y^1 1\delta_+^1 1\bar{\delta}_-^1\rangle+$ $\|1\delta_+^1 1\delta_-^1[(0.50)2\bar{\pi}_x^1 2\pi_y^1+(0.29)2\pi_x^1 2\bar{\pi}_y^1]\rangle$	0.03	0.01	0.20	1.02	1.02	1.0	1.0	1.98	1.76	1.93	1.93
$b\,^3\Phi$	$\|^4G;\ M_L=\pm3\rangle$	$0.51\|2\pi_y^1 1\delta_+^2 1\delta_-^1+2\pi_x^1 1\delta_+^1 1\delta_-^2\rangle-$ $0.41\|2\pi_x^2 2\pi_y^1 1\delta_-^1+2\pi_x^1 2\pi_y^2 1\delta_+^1\rangle$	0.05	0.02	0.29	0.87	0.87	1.10	1.10	1.98	1.78	1.93	1.93
$c\,^3\Sigma^-$	$\|^4P;\ M_L=0\rangle$	$\|(0.65)2\pi_x^1 2\pi_y^1(1\delta_+^2+1\delta_-^2)\rangle$ $+\|(0.27)1\delta_+^1 1\delta_-^1(2\pi_x^2+2\pi_y^2)\rangle$	0.03	0.01	0.20	1.02	1.02	1.0	1.0	1.98	1.76	1.93	1.93
$d\,^3\Pi$	$\|^4D;\ M_L=\pm1\rangle$	$\|(0.55)(2\pi_x^1 1\delta_+^1 1\delta_-^2-2\pi_y^1 1\delta_+^2 1\delta_-^1)\rangle+$ $\|(0.33)3\sigma^1(2\pi_x^1 1\delta_-^2+2\pi_y^1 1\delta_+^2)\rangle$	0.06	0.02	0.50	0.65	0.55	1.25	1.25	1.98	1.79	1.92	1.92
$e\,^3\Delta$	$\|^4D;\ M_L=\pm2\rangle$	$\|1\delta_+^1 1\delta_-^1[(0.86)2\pi_x^1 2\bar{\pi}_y^1-(0.50)2\bar{\pi}_x^1 2\pi_y^1]\rangle$	0.03	0.01	0.20	1.02	1.02	1.00	1.0	1.98	1.76	1.93	1.93
$f\,^3\mathrm{H}$	$\|?;\ M_L=\pm5\rangle$	$(0.50)\|2\pi_x^1(3\sigma^1 1\delta_+^2-3\sigma^1 1\delta_-^2)\rangle-$ $\|2\pi_y^1 1\delta_+^1[(0.57)3\sigma^1 1\bar{\delta}_-^1+(0.35)3\bar{\sigma}^1 1\delta_-^1$	0.10	0.04	1.04	0.54	0.54	1.00	1.0	1.98	1.82	1.92	1.92
$g\,^3\Sigma^+$	$\|^4D;\ M_L=0\rangle$	$\|1\delta_+^1[(0.70)2\bar{\pi}_x^1 2\pi_y^1 1\delta_-^1+(0.41)2\pi_x^1 2\bar{\pi}_y^1 1\delta_-^1-$ $(0.57)2\pi_x^1 2\pi_y^1 1\bar{\delta}_-^1]\rangle$	0.03	0.01	0.20	1.02	1.02	1.00	1.0	1.98	1.76	1.93	1.93
		MnF^+											
$X\,^6\Sigma^+$	$\|^7S;\ M_L=0\rangle$	$0.997\|3\sigma^1 2\pi_x^1 2\pi_y^1 1\delta_+^1 1\delta_-^1\rangle$	0.12	0.04	1.03	1.02	1.02	1.0	1.0	1.97	1.81	1.93	1.93
$a\,^4\Delta$	$\|^5D;\ M_L=\pm2\rangle$	$\|2\pi_x^1 2\pi_y^1 1\delta_-^1[(0.85)1\delta_+^2-(0.31)3\sigma^2]\rangle+$ $\|3\sigma^1 1\delta_+^1 1\delta_-^1[(0.29)2\pi_x^1 2\bar{\pi}_y^1-(0.29)2\bar{\pi}_x^1 2\pi_y^1]\rangle$	0.08	0.03	0.49	1.03	1.03	1.63	1.0	1.98	1.77	1.93	1.93
$b\,^4\Pi$	$\|^5D;\ M_L=\pm1\rangle$	$\|2\pi_y^1 1\delta_+^1 1\delta_-^1[(0.92)2\pi_x^2-(0.31)3\sigma^2]\rangle$	0.07	0.03	0.38	1.79	1.79	0.98	0.98	1.98	1.77	1.94	1.94
$c\,^4\Phi$	$\|^5G;\ M_L=\pm3\rangle$	$\|(0.60)3\sigma^1(2\pi_x^1 1\delta_+^1 1\delta_-^2-2\pi_y^1 1\delta_+^2 1\delta_-^1)\rangle+$ $\|(0.37)3\sigma^1(2\pi_x^2 2\pi_y^1 1\delta_-^1-2\pi_x^1 2\pi_y^2 1\delta_+^1)\rangle$	0.10	0.04	1.15	0.53	0.65	1.39	1.39	1.99	1.82	1.92	1.92
$d\,^4\Sigma^+$	$\|^5S;\ M_L=0\rangle$	$0.70\|3\sigma^1 1\delta_+^1 2\bar{\pi}_x^1 2\pi_y^1 1\delta_-^1\rangle+$ $\|(0.50)2\pi_x^1 1\delta_+^1 1\delta_-^1(3\sigma^1 2\bar{\pi}_y^1-3\bar{\sigma}^1 2\pi_y^1)\rangle$	0.11	0.04	1.05	1.03	1.03	1.0	1.0	1.98	1.80	1.94	1.94
$e\,^4\Pi$	$\|^5G;\ M_L=\pm1\rangle$	$\|(0.63)3\sigma^1(2\pi_y^1 1\delta_+^2 1\delta_-^1+2\pi_x^1 1\delta_+^1 1\delta_-^2)\rangle+$ $0.39\|3\sigma^2 2\pi_y^1 1\delta_+^1 1\delta_-^1\rangle$	0.10	0.04	1.15	0.53	0.65	1.39	1.39	1.99	1.82	1.92	1.92
$f\,^4\Gamma$	$\|^5G;\ M_L=\pm4\rangle$	$0.79\|3\sigma^1 2\pi_x^1 2\pi_y^1 1\delta_+^1 1\bar{\delta}_-^1\rangle+$ $\|2\pi_y^1 1\delta_-^1[(0.50)3\bar{\sigma}^1 2\pi_x^1 1\delta_+^1+(0.29)3\sigma^1 2\bar{\pi}_x^1 1\delta_+^1]\rangle$	0.12	0.04	1.04	1.02	1.02	1.0	1.0	1.98	1.80	1.94	1.94

degenerate within each group. Numerical results in a variety of methods are given in Table VIII and asymptotic limits and Mulliken electron distributions in Fig. 6 and Table IX.

B. The anions MF^-

No experimental or theoretical results exist in the literature on the anionic MF^- series, M = Sc to Mn. The experimental EAs of Sc, Ti, V, Cr, and Mn are 0.188 ± 0.02, 0.079 ± 0.014, 0.525 ± 0.012, 0.666 ± 0.012, and <0 eV, respectively.[39] The EA of F is 3.40 eV,[35] hence the end fragments of MF^- are certainly $M+F^-(^1S)$. From the asymptotic products it is rather clear that the most efficient approach for calculating the $M+F^-$ interactions, even to construct full potential energy curves, is the coupled cluster method. In addition, the EA of F atom is calculated to be

3.38 eV at the RCCSD(T)/AQZ level in excellent agreement with experiment, a crucial quantity for the accurate description of the $M\mathrm{F}^-$s.

Our coupled-cluster calculations predict surprisingly high binding energies ranging from 76 (ScF^-) to 50 (CrF^-) kcal/mol at the RCCSD(T) level (*vide infra*), and adiabatic EAs ($M\mathrm{F}+e^-\rightarrow M\mathrm{F}^-$) of about 1 eV; in other words we are dealing with quite stable chemical systems. However, we are confronted with a conceptual problem, i.e., the nature of the $M\cdots\mathrm{F}^-$ bond; what is its character? Let us take as an example the TiF^- anion. Consider the valence-bond Lewis diagram of the ground state neutral TiF at equilibrium, $\mathrm{Ti}^+\mathrm{F}^-$; Ref. 1.

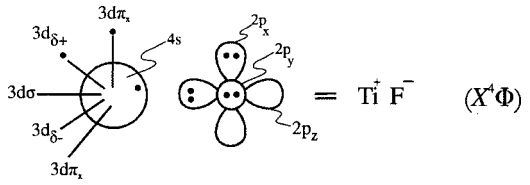

$\mathrm{Ti}^+(^4\mathrm{F};\mathrm{M_L}=\pm 3)\ \ \mathrm{F}^-(^1\mathrm{S})$

By attaching one e^- to the Ti^+ end of the neutral TiF $=\mathrm{Ti}^+$ $(3d^24s^1;{}^4F)-\mathrm{F}^-$, the positive charge on the metal atom is practically quenched, resulting to the ground $^3\Phi$ state of the $\mathrm{Ti}(3d^24s^2;{}^3F)-\mathrm{F}^-$ anion. We can imagine the formation of the other four $M\mathrm{F}^-$s in the same fashion: From the X states of Sc^+ $(3d^14s^1;{}^1D)-\mathrm{F}^-$ $[^1\Sigma^+]$, V^+ $(3d^34s^1;{}^5F)-\mathrm{F}^-$ $[^5\Pi]$, Cr^+ $(3d^44s^1;{}^6D)-\mathrm{F}^-$ $[^6\Sigma^+]$, and Mn^+ $(3d^54s^1;{}^7S)-\mathrm{F}^-$ $[^7\Sigma^+]$,[1] the ground state anions $\mathrm{Sc}(3d^14s^2;{}^2D)-\mathrm{F}^-$ $[^2\Delta]$, $\mathrm{V}(3d^34s^2;{}^4F)-\mathrm{F}^-$ $[^4\Delta$ or $^4\Pi]$, $\mathrm{Cr}(3d^54s^1;{}^7S)-\mathrm{F}^-$ $[^7\Sigma^+]$, and $\mathrm{Mn}(3d^54s^2;{}^6S)-\mathrm{F}^-$ $[^6\Sigma^+]$ result, respectively. Note that all the *in situ* metal atoms find themselves in their ground state, carrying a Hartree–Fock Mulliken charge of about $0.3e^-$ (*vide infra*).

Another formation channel of the $M\mathrm{F}^-$ X states, at least for the ScF^-, TiF^- and VF^- anions, could entail the first excited high spin state of the metal atom, i.e., $\mathrm{Sc}(3d^24s^1;{}^4F)$, $\mathrm{Ti}(3d^34s^1;{}^5F)$, and $\mathrm{V}(3d^44s^1;{}^6D)$, respectively. Indeed, strongly bound states emanate from these metal terms but they do not seem to be the ground states; their binding energies cannot overcome the additional splittings[9] $\mathrm{Sc}(^4F\leftarrow{}^2D)=1.43$ (1.63) eV, $\mathrm{Ti}(^5F\leftarrow{}^3F)=0.80$ (0.92) eV, and $\mathrm{V}(^6D\leftarrow{}^4F)=0.25$ (0.30) eV [RCCSD(T) values in parenthesis] and become the ground states.

The following $M\mathrm{F}^-$ states accessible by the coupled-cluster method have been examined. ScF^-: $X\,^2\Delta$, $A\,^2\Pi$, $B\,^2\Sigma^+$, and $a\,^4\Sigma^+$; TiF^-: $X\,^3\Phi$, $A^3\Sigma^-$, $B^3\Delta$, $a\,^5\Delta$, and $\mathrm{b}\,^5\Phi$; VF^-: $X\,^4\Delta$, $A\,^4\Pi$, and $a\,^6\Sigma^+$; CrF^-: $X\,^7\Sigma^+$; MnF^-: $X\,^6\Sigma^+$.

Table X summarizes all our numerical findings in the $M\mathrm{F}^-$ series, while Figs. 7–11 present PECs at the RCCSD(T) level of theory.

1. ScF⁻

The three calculated doublets of ScF^-, $X\,^2\Delta$, $A\,^2\Pi$, and $B\,^2\Sigma^+$ correlate to the ground state of Sc (^2D). These states result from the lifting of degeneracy of the ^2D term in the presence of the F^- field. The Hartree–Fock configurations of the three doublets are $|X\,^2\Delta(A\,^2\Pi)[B\,^2\Sigma^+]\rangle$ $=|\{(\mathrm{core})^{20}1\sigma^22\sigma^23\sigma^21\pi_x^21\pi_y^2\}1\delta_+^1(2\pi_x^1)[4\sigma^1]\rangle$. About $0.25e^-$ are transferred from the F^- to the Sc atom, mainly to its $4p_z$ orbital in the $X\,^2\Delta$, $A\,^2\Pi$, and $B\,^2\Sigma^+$ states according to the Hartree–Fock (HF) Mulliken distributions. This rather small electron transfer can be considered as the cause of relatively high binding energies, 85 ($X\,^2\Delta$), 74 ($A\,^2\Pi$), and 70 ($B\,^2\Sigma^+$) kcal/mol at the C-RCCSD(T) level and practically identical equilibrium bond lengths.

The situation for the $a\,^4\Sigma^-$ is a little bit different. Adiabatically, it correlates to the first excited state of Sc ($3d^24s^1;{}^4F$), 1.43 eV above the ^2D term.[9] However, the HF equilibrium Mulliken distributions (Sc/F) $4s^{0.89}4p_z^{0.11}4p_x^{0.60}4p_y^{0.60}3d_{z^2}^{0.12}3d_{xz}^{0.41}3d_{yz}^{0.41}/2s^{1.99}2p_z^{1.88}2p_x^{1.98}2p_y^{1.98}$ indicate that the *in situ* Sc correlates *diabatically* to a $3d^14s^14p^1$ (^4F) configuration, 1.956 eV higher than the ^2D state.[9] According to the populations above the $3d^14s^14p^1$ (^4F) electrons on Sc are redistributed at equilibrium to three hybrids, namely, $(4s3d_{z^2})^{1.01}$, $(4p_x3d_{xz})^{1.01}$, and $(4p_y3d_{yz})^{1.01}$, while $0.11e^-$ are transferred from the $2p_z$ of F^- to the empty $4p_z$ orbital of Sc. The result is a remarkably strong binding energy of 89 kcal/mol [C-RCCSD(T)] with respect to Sc $(3d^24s^1;{}^4F)+\mathrm{F}^-(^1S)$, and a shorter bond length as compared to the doublets.

2. TiF⁻

In the presence of the F^- field we expect the formation of four low-lying molecular triplets, i.e., $^3\Sigma^-$, $^3\Pi$, $^3\Delta$, and $^3\Phi$ correlating to the ground state Ti atom, ^3F $(3d^24s^2)$. We did not calculate the $^3\Pi$ state because of its intense multireference character. We have also examined two quintets, $^5\Delta$ and $^5\Phi$, correlating adiabatically to the first excited state of Ti $(3d^34s^1;{}^5F)$ located 0.80 eV higher.[9] The HF configurations of the three triplets are

$$|X\,^3\Phi(A^3\Sigma^-)[^3\Delta]\rangle=|\{(\mathrm{core})^{20}1\sigma^22\sigma^23\sigma^21\pi_x^21\pi_y^2\}\times 2\pi_x^11\delta_+^1(1\delta_+^11\delta_-^1)[4\sigma^11\delta_+^1]\rangle.$$

The HF equilibrium Mulliken populations indicate that $0.33e^-$, $0.36e^-$, and $0.33e^-$ are transferred from the $2s2p_z$ F^- orbitals, mainly to the $4p_z$ and $3d_{z^2}$ orbitals of the Ti atom for the $X\,^3\Phi$, $A\,^3\Sigma^-$, and $^3\Delta$ states, respectively. Binding energies and bond lengths are similar to the ScF^- doublets, the highest D_e being 77 kcal/mol at the C-RCCSD(T) level. Note that the ground state has been only formally assigned as $^3\Phi$; the $^3\Sigma^-$ state is less than 1 kcal higher at the C-RCCSD(T) level but shows a tendency to become the X state after the DK corrections.

The PECs of the triplets depicted in Fig. 8 show the inability of the single reference RCCSD(T) method to describe sufficiently well the Ti atom at infinity $(3d^24s^2,{}^3F;M=0)$ in the $A\,^3\Sigma^-$ state.

The HF configurations of the $^5\Delta$ and $^5\Phi$ states are the following: $|^5\Delta(^5\Phi)\rangle=|\{(\mathrm{core})^{20}1\sigma^22\sigma^23\sigma^11\pi_x^21\pi_y^2\}2\pi_x^1 2\pi_y^11\delta_+^1(4\sigma^12\pi_x^11\delta_+^1)\rangle$. A total charge of 0.17 ($^5\Delta$) and 0.15 ($^5\Phi$) e^- migrates from the $2p_z$ orbital of F^- to the $4p_z$ orbital of the Ti atom, giving rise to binding energies of 77 and 69 kcal/mol.

TABLE X. Total energies E (hartree), equilibrium bond distances r_e (Å), dissociation energies D_e (kcal/mol), harmonic/anharmonic frequencies $\omega_e/\omega_e x_e$ (cm^{-1}), and energy separations T_e (cm^{-1}) for the MF^- series, M = Sc, Ti, V, Cr, and Mn.

Method	$-E$	r_e	D_e	ω_e	$\omega_e x_e$	T_e
			ScF^-			
			$X\ ^2\Delta$			
RCCSD(T)	859.678 11	2.072	76.3	541	6.4	0.0
RCCSD(T)+DK	863.312 91	2.069	76.3			0.0
C-RCCSD(T)	859.981 62	1.912	85.4	567	3.3	0.0
C-RCCSD(T)+DK	863.664 56	1.912	83.9			0.0
			$A\ ^2\Pi$			
RCCSD(T)	859.663 48	2.084	67.2	523	7.0	3212
RCCSD(T)+DK	863.298 94	2.073	67.6			3064
C-RCCSD(T)	859.964 06	1.928	74.4	509	5.3	3855
C-RCCSD(T)+DK	863.647 59	1.918	73.3			3725
			$B\ ^2\Sigma^+$			
RCCSD(T)	859.657 12	2.058	63.2	468	5.9	4607
C-RCCSD(T)	859.957 10	1.912	70.1	478	3.5	5381
			$a\ ^4\Sigma^-$			
RCCSD(T)	859.635 98	2.004	87.7	509	3.0	9246
C-RCCSD(T)	859.932 70	1.900	89.4	555	3.7	10737
			TiF^-			
			$X\ ^3\Phi$			
RCCSD(T)	948.360 43	1.934	74.5	550	4.0	0.0
RCCSD(T)+DK	952.783 96	1.929	74.4			0.0
C-RCCSD(T)	948.680 53	1.896	77.4	556	3.6	0.0
C-RCCSD(T)+DK	953.154 69	1.890	74.8			0.0
			$A\ ^3\Sigma^-$			
RCCSD(T)	948.358 78	1.894	73.4	575	4.4	362
RCCSD(T)+DK	952.782 61	1.889	73.5			297
C-RCCSD(T)	948.679 52	1.837	76.8	617	3.8	221
C-RCCSD(T)+DK	953.154 92	1.835	74.9			−50
			$B\ ^3\Delta$			
RCCSD(T)	948.348 17	1.964	66.8	503	3.8	2691
RCCSD(T)+DK	952.772 56	1.952	67.2			2503
C-RCCSD(T)	948.667 63	1.923	69.3	512	3.3	2831
C-RCCSD(T)+DK	953.143 68	1.915	67.9			2416
			$a\ ^5\Delta$			
RCCSD(T)	948.330 27	1.916	76.8			6619
			$b\ ^5\Phi$			
RCCSD(T)	948.318 53	1.940	69.4			9194
			VF^-			
			$X\ ^4\Delta$			
RCCSD(T)	1042.859 19	1.905	72.4	547	4.2	0.0
C-RCCSD(T)	1043.199 68	1.886	74.7	560	4.0	0.0
			$A\ ^4\Pi$			
RCCSD(T)	1042.857 06	1.905	71.1	547	4.0	467
C-RCCSD(T)	1043.199 63	1.886	74.7	561	4.5	11
			$a\ ^6\Sigma^+$			
RCCSD(T)	1042.837 37	1.889	65.5	490	2.8	4789
C-RCCSD(T)	1043.182 51	1.883	66.3	476		3768
			CrF^-			
			$X\ ^7\Sigma^+$			
RCCSD(T)	1143.322 22	1.964	50.4	443	3.4	0.0
C-RCCSD(T)	1143.682 51	1.952	51.8	466		0.0
C-RCCSD(T)+DK	1150.121 65	1.934	51.6			0.0
			MnF^-			
			$X\ ^6\Sigma^+$			
RCCSD(T)	1249.880 78	1.922	56.6	492	3.9	0.0
RCCSD(T)+DK	1257.480 26	1.917	55.9			
C-RCCSD(T)	1250.241 46	1.908	58.3	494		
C-RCCSD(T)+DK	1257.898 70	1.911	55.4			

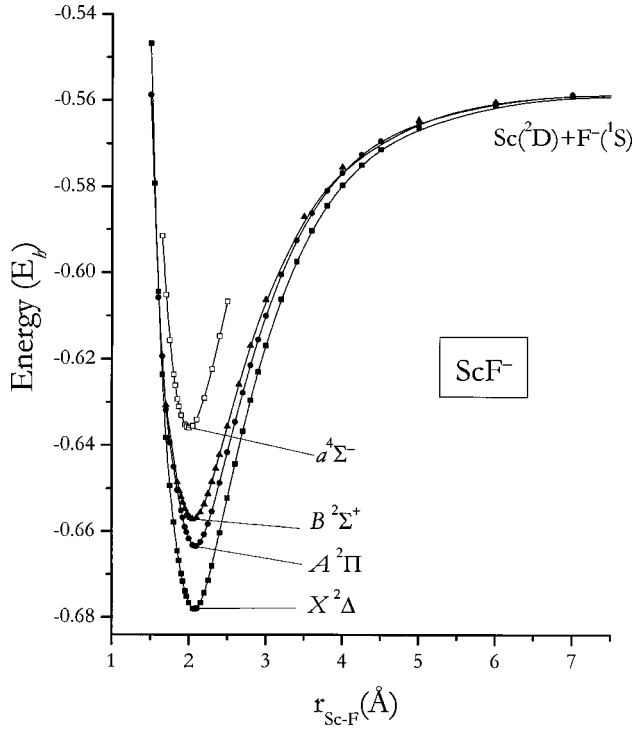

FIG. 7. RCCSD(T)/(ANO/AQZ) potential energy curves of $X\,^2\Delta$, $A\,^2\Pi$, $B\,^2\Sigma^+$, and $a\,^4\Sigma^-$ states of ScF^-. Energies shifted by $+859E_h$.

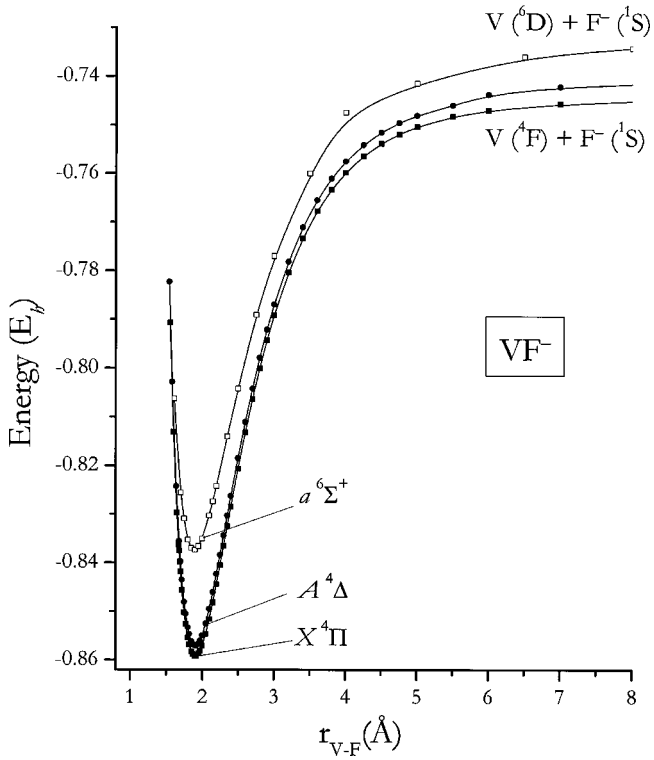

FIG. 9. RCCSD(T) PECs of $X\,^4\Pi$, $A\,^4\Delta$, and $a\,^6\Sigma^-$ states of VF^-. Energies shifted by $+1042E_h$.

3. VF^-

From the Σ^-, Π, Δ, and Φ quartets originating from the ^4F ($3d^34s^2$) state of V we examined the $^4\Delta$ and $^4\Pi$ states and a sextet, $^6\Sigma^+$, correlating to the first excited state of V($3d^44s^1$; ^6D), 0.25 eV (Ref. 9) above the ^4F term. According to Table X the two quartets are strictly degenerate at the C-RCCSD(T) level and with PECs of identical morphology, as reflected in the r_e, ω_e, and $\omega_e x_e$ values, Fig. 9.

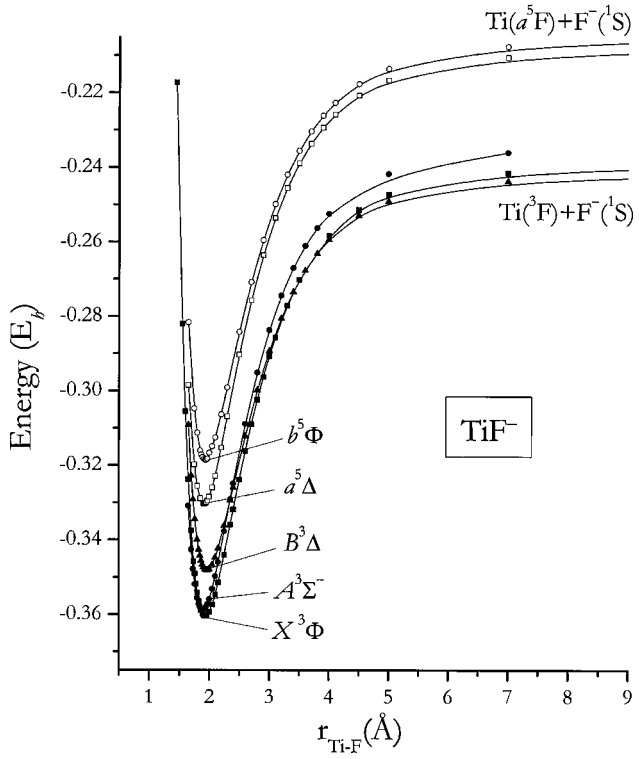

FIG. 8. RCCSD(T) PECs of $X\,^3\Phi$, $A\,^3\Sigma^-$, $B\,^3\Delta$, $a\,^5\Delta$, and $b\,^5\Phi$ states of TiF^-. Energies shifted by $+948E_h$.

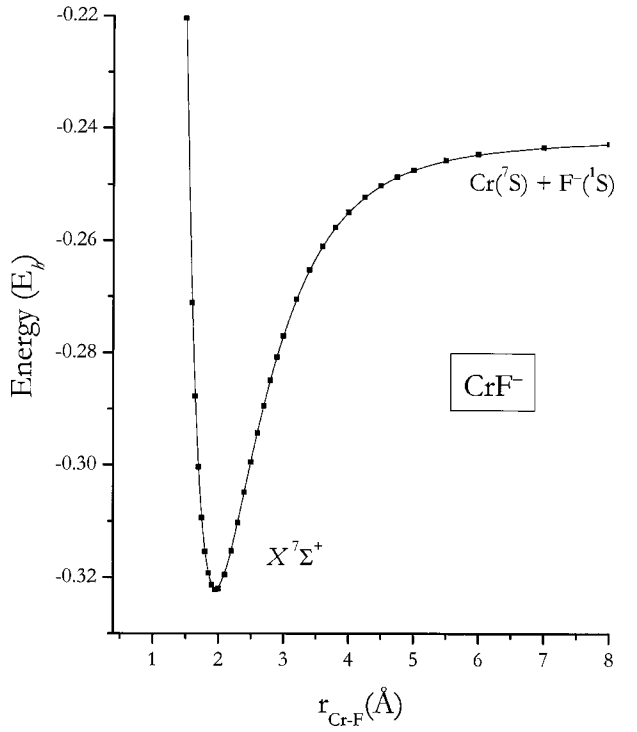

FIG. 10. RCCSD(T) PEC of the $X\,^7\Sigma^+$ state of CrF^-. Energies shifted by $+1143E_h$.

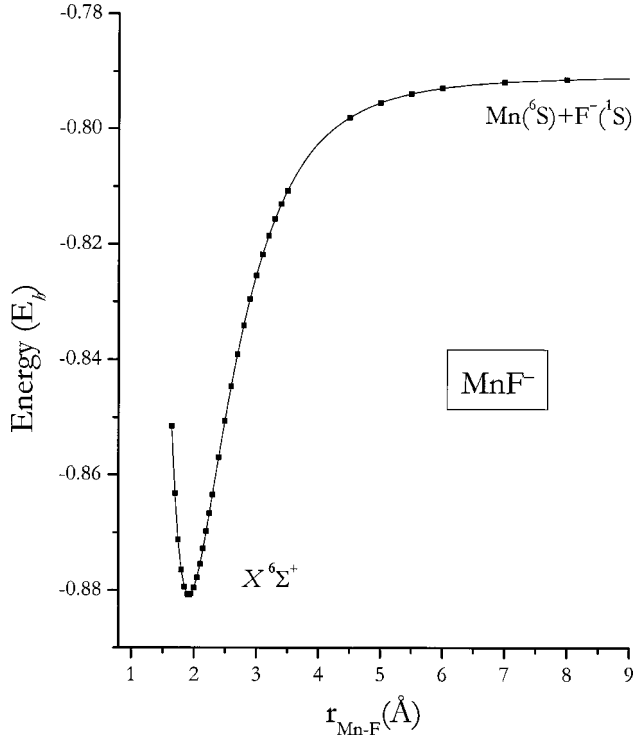

FIG. 11. RCCSD(T) PEC of the $X\,^6\Sigma^+$ state of MnF^-. Energies shifted by $+1249E_h$.

Obviously the X and A tagging is purely formal. The HF configurations of $^4\Delta$ and $^4\Pi$ states are

$$|^4\Delta(^4\Pi)\rangle = |\{(\text{core})^{20}1\sigma^2 2\sigma^2 3\sigma^2 1\pi_x^2 1\pi_y^2\} \times 2\pi_x^1 2\pi_y^1 1\delta_-^1 (2\pi_y^1 1\delta_+^1 1\delta_-^1)\rangle.$$

In both states about $0.4e^-$ are dispersed from the $2s2p_z$ orbitals of the F^- anion to the σ frame of the V atom.

4. CrF⁻ and MnF⁻

We have calculated the $X\,^7\Sigma^+$ $\{=|(\text{core})^{20}1\sigma^2 2\sigma^2 3\sigma^1 4\sigma^1 1\pi_x^2 2\pi_x^1 1\pi_y^2 2\pi_y^1 1\delta_+^1 1\delta_-^1\rangle\}$ and $X\,^6\Sigma^+$ $\{=|(\text{core})^{20}1\sigma^2 2\sigma^2 3\sigma^2 4\sigma^1 1\pi_x^2 2\pi_x^1 1\pi_y^2 2\pi_y^1 1\delta_+^1 1\delta_-^1\rangle\}$ states of CrF^- and MnF^-, correlating to Cr $(3d^5 4s^1; {}^7S)$ and Mn $(3d^5 4s^2; {}^6S) + F^-({}^1S)$, respectively. Their PECs are shown in Figs. 10 and 11.

In CrF^- $0.24e^-$ migrate from the $2s2p_z$ orbitals of F^-, mainly to the $4p_z$ orbital of the Cr atom, while in MnF^- about $0.4e^-$ are transferred from the $2s2p_z$ orbitals of F^- atom to the $4p_z5s$ σ-frame orbitals of Mn. C-RCCSD(T) binding energies are 52 and 58 kcal/mol for the CrF^- and MnF^-, respectively.

V. SUMMARY AND FINAL REMARKS

We have examined the electronic structure of the charged diatomic fluorides $MF^\pm$, M=Sc, Ti, V, Cr, and Mn using multireference configuration interaction and coupled-cluster techniques, in combination with extensive basis sets. Note that ScF^+, VF^+, and MnF^+ as well as all five anions MF^-, M=Sc to Mn, have never been investigated before either experimentally or theoretically. In a recent publication we investigated the electronic structure of the neutral fluorides MF, M=Ti to Mn, using identical methods and basis sets.[1] For reasons of completeness and/or comparison, we also studied presently two states ($X\,^1\Sigma^+$, $a\,^3\Delta$) of the first member of the neutral sequence, ScF. A total of 29 and 14 states were examined for the MF^+ and MF^- species, respectively. For almost all states we have constructed full MRCI (MF^+ and ScF) and RCCSD(T) (MF^-) potential energy curves, reporting total energies, dissociation energies and the usual spectroscopic parameters (r_e, ω_e, $\omega_e x_e$, and α_e). The effects of special relativity were taken into account via the Douglas-Kroll approximation.

TABLE XI. Estimated dissociation energies D_e, bond distances r_e, and ionization energies IE of the X states of the $MF^{\pm1,0}$ species, M=Sc, Ti, V, Cr, and Mn.

Species[a]	X state	D_e[b] (kcal/mol)	r_e (Å)	IE (eV)
ScF	$^1\Sigma^+$	144	1.790	6.6±0.1
ScF^+	$^2\Delta$	140	1.795	
ScF^-	$^2\Delta$	85	1.912	0.75±0.05
TiF	$^4\Phi$	135	1.837	6.8±0.1
TiF^+	$^3\Sigma^-/{}^3\Phi$[c]	130	1.734[d]/1.775	
TiF^-	$^3\Sigma^-/{}^3\Phi$[c]	77	1.835/1.890	1.0
VF	$^5\Pi$	130	1.788	7.2±0.1
VF^+	$^4\Pi$	116	1.734	
VF^-	$^4\Delta/{}^4\Pi$[c]	75	1.886	0.92
CrF	$^6\Sigma^+$	110	1.783	7.7±0.1
CrF^+	$^5\Sigma^+$	87	1.722	
CrF^-	$^7\Sigma^+$	52	1.952	0.71
MnF	$^7\Sigma^+$	108	1.840	8.0±0.1
MnF^+	$^6\Sigma^+$	92	1.750	
MnF^-	$^6\Sigma^+$	58	1.908	1.13

[a]Neutral MFs, M=Ti to Mn from Ref. 1; ScF present work.
[b]With respect to adiabatic fragments.
[c]Degenerate states within the accuracy of our calculations, see text.
[d]Averaged C-MRCI+DK+Q and C-RCCSD(T) values using the C5Z/A5Z basis set.

Table XI is a short and useful summary of r_e and D_e values of the ground states of the entire $MF^{\pm1,0}$ series, including the adiabatic IEs of the neutrals ($MF \rightarrow MF^+ + e^-$) and the anions ($MF^- \rightarrow MF + e^-$), or the EAs of the former. A few general conclusions can be drawn from Table XI:

(a) $D_e(MF) > D_e(MF^+) > D_e(MF^-)$, M=Sc to Mn.
(b) The D_e values of the $MFs^{\pm1,0}$ decrease monotonically as we move from Sc to Cr, where they present a minimum [with the exception of CrF where $D_e(\text{CrF}) = D_e(\text{MnF}) + 2$ kcal/mol].
(c) The EAs of MFs (or the IEs of MFs^-) are more or less constant across the Sc to Mn series and about 1 eV.
(d) The IEs of the MF neutrals increase monotonically as we move from Sc to Mn ranging from 6.8 (ScF) to 8.0 (MnF) eV.

These findings are shown graphically in Fig. 12 along with the theoretical and experimental IEs of the M atoms, Sc to Mn.

The main conclusion for the MF^+ cations is that they are almost as ionic as the corresponding neutrals; in all species and states studied a Mulliken charge transfer is observed from M^+ to F of about $0.65e^-$. Therefore, their equilibrium

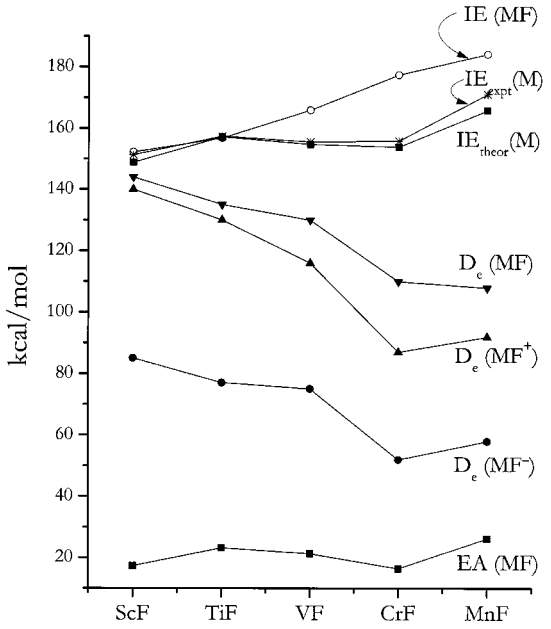

FIG. 12. Ground state dissociation energies D_e of $MF^{\pm 1,0}$, electron affinities EA and ionization energies IE of MFs, and theoretical and experimental IEs of the M atoms, $M=$ Sc, Ti, V, Cr, and Mn.

can be described fairly well as $M^{2+}F^-$. As in the case of neutrals the PECs of the cations for the internuclear distance $2.6 \leqslant r \leqslant 5$ bohr, can be fitted remarkably well to a Rittner-type potential[40]

$$V(r) = -\frac{1}{r} - \frac{A}{r^4} + Be^{-r/C},$$

where, A, B, and C are freely adjustable parameters. This is, indeed, an independent indication of the ionic bonding character of these species; see also Ref. 1.

Although experimentally the TiF^+ ground state is of $^3\Phi$ symmetry, our calculations indicate that a $^3\Sigma^-$ state cannot be ruled out.

The ground states of ScF^-, CrF^-, and MnF^- are of $^2\Delta$, $^7\Sigma^+$, and $^6\Sigma^+$ symmetries, respectively, but we cannot be sure for the ground states of TiF^- ($^3\Sigma^-$ or $^3\Phi$) and VF^- ($^4\Delta$ or $^4\Pi$). Although the D_e values of the MF^-s are about half of the corresponding neutrals, yet they can be considered as ''strongly'' bound, their binding energies ranging from 85 (ScF^-) to 52 (CrF^-) kcal/mol (Table XI). It should be said at this point that we are not sure as to the bonding nature of the MF^- anions. The bonding results by the ''dispersion'' of $0.2e^- - 0.4e^-$ according to the Mulliken analysis, along the σ-frame and with the *in situ* M atoms appearing negatively charged accordingly.

Perhaps we can come to terms with the high binding energies of the MF^- systems by using an electrostatic (classical) interpretation. The transition metal atoms have large static polarizabilities (α) which (in Å^3) are $\sim$17.8, 14.6, 12.4, 11.6, and 9.4 for the sequence Sc to Mn.[41] The negatively charged F atom will polarize the metal and if the *in situ* F charge is $-q$ the induction energy will be $-(q^2\alpha/2r^4)$ (Ref. 42), or $-(q^2\alpha/2r^4)+(q(1-q)/r)$ correcting for the Coulombic repulsion, where r is the distance between the two negatively charged species F^{q-}, $M^{-(1-q)}$. Using the $r=r_e$ bond distances (Table XI) and $q\approx 0.7$ one obtains (in kcal/mol) -72, -67, -43, -29, and -21 for the MF^-, $M=$ Sc to Mn series. Although the agreement cannot be considered as ''striking,'' nevertheless it is interesting. Within the approximate values of α' s and q's the model predicts correctly a diminishing binding energy along the sequence Sc to Mn, and gives a satisfactory feeling on the order of the interaction energy.

Finally, in an effort to understand better the anions we examined the $^3\Phi$ state of the Ti–Ne molecule, isoelectronic to TiF^-, at the C-RCCSD(T)/($C5Z_{Ti}/A5Z_{Ne}$) level of theory. The TiNe system is purely repulsive with a van der Waals interaction energy of $-E$ (vdW)$=17.3-3.9$ (BSSE) $cm^{-1}=13.4\ cm^{-1}$, at $r_{vdW}=5.0$ Å. Clearly, what makes the difference between the F^- and the rare gas Ne as to their bonding ability to the M atoms, is their IEs, 3.40 and 21.6 eV,[9] respectively, i.e., their propensity to donate electrons coupled with the very large polarizabilities of the M atoms.

ACKNOWLEDGMENTS

The authors acknowledge the National and Kapodistrian University of Athens for financial support through its Special Research Account for Basic Research. S.K. and C.K. express their gratitude to the Hellenic State Scholarship Foundation (IKY) for financial support. The computing time provided by the National Center for Scientific Research, DEMOKRITOS, is greatly appreciated. We also thank the reviewer for his (her) suggestion concerning the electrostatic interpretation of the MF-binding energies.

[1] C. Koukounas, S. Kardahakis, and A. Mavridis, J. Chem. Phys. **120**, 11500 (2004), and references therein.
[2] J. F. Harrison, Chem. Rev. (Washington, D.C.) **100**, 679 (2000), and references therein.
[3] T. Pradeep, D. E. Riederer, Jr., S. H. Hoke II, T. Ast, R. G. Cooks, and M. R. Linford, J. Am. Chem. Soc. **116**, 8658 (1994).
[4] C. Focsa, B. Pinchemel, D. Collet, and T. R. Huet, J. Mol. Spectrosc. **189**, 254 (1998).
[5] D. Schröder, J. N. Harvey, and H. Schwarz, J. Phys. Chem. A **102**, 3639 (1998).
[6] J. W. Hastie and J. L. Margrave, in *Fluorine Chemistry Reviews*, edited by P. Tarrant (Dekker, New York, 1968), Vol. 2, p. 102.
[7] C. Focsa and B. Pinchemel, Chem. Phys. **247**, 395 (1999).
[8] R. A. Kent and J. L. Margrave, J. Am. Chem. Soc. **87**, 3582 (1965).
[9] C. A. Moore, *Atomic Energy Levels*, Natl. Bur. Stand. (U.S.) Circ. No. 35 (U.S. GPO, Washington, D.C., 1971).
[10] J. F. Harrison, J. Phys. Chem. **90**, 3313 (1986).
[11] C. W. Bauschlicher, Jr., Theor. Chim. Acta **92**, 183 (1995).
[12] T. H. Dunning, Jr., J. Chem. Phys. **90**, 1007 (1989); R. A. Kendall, T. H. Dunning, Jr., and R. J. Harrison, *ibid.* **96**, 6796 (1992).
[13] C. W. Bauschlicher, Jr., Theor. Chem. Acc. **103**, 141 (1999).
[14] MOLPRO 2000, version 2002.6, is a package of *ab initio* programs designed by H.-J. Werner, P. J. Knowles, R. D. Amos *et al.*
[15] ACESII is a program product of Quantum Theory Project, University of Florida, J. F. Stanton, J. Gauss, J. D. Watts *et al.* Integral packages included are VMOL (J. Almlöf and P. R. Taylor); VPROPS (P. R. Taylor); and ABACUS (T. Helgaker, H. J. Aa. Jensen, P. Jørgensen, J. Olsen, and P. R. Taylor).
[16] M. Douglas and N. M. Kroll, Ann. Phys. (N.Y.) **82**, 89 (1974); B. A. Hess, Phys. Rev. A **32**, 756 (1985); **33**, 3742 (1986).
[17] R. J. Gdanitz and R. Ahlrichs, Chem. Phys. Lett. **143**, 413 (1988); H.-J. Werner and P. J. Knowles, Theor. Chim. Acta **84**, 95 (1992).
[18] K. Docken and J. Hinze, J. Chem. Phys. **57**, 4928 (1972); H.-J. Werner and W. Meyer, *ibid.* **74**, 5794 (1981).

[19] K. F. Zmbov and J. L. Margrave, J. Chem. Phys. **47**, 3122 (1967).
[20] D. L. Hildenbrand and K. H. Lau, J. Chem. Phys. **102**, 3769 (1995).
[21] E. A. Shenyavskaya, A. J. Ross, A. Topouzkhanian, and G. Wannous, J. Mol. Spectrosc. **162**, 327 (1993).
[22] B. Simard, M. Vasseur, and P. A. Hackett, Chem. Phys. Lett. **176**, 303 (1991).
[23] E. A. Shenyavskaya, M.-A. Lebault-Dorget, C. Effantin, J. D' Incan, A. Bernard, and J. Vergès, J. Mol. Spectrosc. **171**, 309 (1995).
[24] K. D. Carlson and C. Moser, J. Chem. Phys. **46**, 35 (1967).
[25] J. F. Harrison, J. Phys. Chem. **87**, 1312 (1983).
[26] S. R. Langhoff, C. W. Bauschlicher, Jr., and H. Partridge, J. Chem. Phys. **89**, 396 (1988).
[27] R. Ahlrichs, P. Scharf, and C. Ehrhardt, J. Chem. Phys. **82**, 890 (1985).
[28] K. F. Zmbov and J. L. Margrave, J. Phys. Chem. **71**, 2893 (1967).
[29] R. S. Ram, J. R. D. Peers, Y. Teng, A. G. Adam, A. Muntianu, P. F. Bernath, and S. P. Davis, J. Mol. Spectrosc. **184**, 186 (1997).
[30] R. S. Ram, P. F. Bernath, and S. P. Davis, J. Chem. Phys. **116**, 7035 (2002).
[31] O. Launila, J. Mol. Spectrosc. **169**, 373 (1995).
[32] T. C. Devore and J. L. Gole, J. Phys. Chem. **100**, 5660 (1996).
[33] G. Balducci, M. Campodonico, G. Gigli, G. Meloni, and S. N. Cesaro, J. Chem. Phys. **117**, 10613 (2002).
[34] O. Launila, B. Simard, and A. M. James, J. Mol. Spectrosc. **159**, 161 (1993).
[35] A. Chrissanthopoulos and G. Maroulis, J. Phys. B **34**, 121 (2001).
[36] D. Tzeli and A. Mavridis, J. Chem. Phys. **118**, 4984 (2003).
[37] C. Blondel, Phys. Scr. **58**, 31 (1995).
[38] A. Kent, T. C. Ehlert, and J. L. Margrave, J. Am. Chem. Soc. **86**, 5090 (1964).
[39] H. Hotop and W. C. Lineberger, J. Phys. Chem. Ref. Data **14**, 731 (1985).
[40] E. S. Rittner, J. Chem. Phys. **19**, 1030 (1951).
[41] G. D. Doolen, in *Handbook of Chemistry and Physics*, 83rd ed., edited by D. R. Lide (CRC, New York, DC, 2002).
[42] A. J. Stone, *The Theory of Intermolecular Forces* (Clarendon, Oxford, 1996), p. 54.